SPS

programme de recherche

Publication de l'Antenne 35

GIS AND REMOTE SENSING FOR MAPPING SOILS AND EROSION HAZARD IN THE KAYA REGION, BURKINA FASO

M. A. Mulders, S. Sorateyan

Preliminary Results of Processing Terrain and Remote Sensing Data of the Zablou Area (Burkina Faso)

M.A. Mulders, A. Casterad

Deriving Sub-Pixel Soil Characteristics in Northern Burkina Faso with Spectral Unmixing

M. Tromp, M.Z. Steenis

Getting Insight into Soils and Land with M.A.S.I.S. : a Proposed Methodology in a Remote Sensing - GIS Environment: a Case Study of the Manga Area, Burkina Faso

T. Laguna Gomez

Excursion to the Kaya Region, burkina Faso

P.N. Zombré et. al.

In: Proceedings of the ISSS congress on GIS and Remote Sensing, Ouagadougou, 1995

Aménagement et Gestion
e Sylvo-Pastoral au Sahel

lienne de l'Université Agronomique Wageningen Pays-Bas
sité de Ouagadougou Burkina Faso

GIS and Remote Sensing for Mapping Soils and Erosion Hazard in the Kaya Region, Burkina Faso

M.A. MULDERS, S. SORATEYAN

Wageningen Agricultural University, Soil Science and Geology, POB 37, 6700 AA Wageningen, The Netherlands.

Abstract

Interpretations of TM satellite data and of aerial photographs are important tools for soil mapping. They enable planning of the field survey by directing the observations to the most informative sites. GIS enables control on validity of interpretation units for selected terrain characteristics as well as a check on accuracy of boundaries of mapping units by studying the relationship of spectral information with specific terrain data.

It also provides for a powerful instrument to compose useful combinations of thematic data and evaluate their informative value.

In this study, schemes were made on information acquisition, reconnaissance soil mapping and erosion hazard mapping in a second phase, using remote sensing, GIS and dBase.

During the fieldwork at scale 1:30,000 of the second phase, emphasis was laid upon filling up gaps in observation on soils. A land use map was constructed and observations were done to build up a terrain database according to the SOTER system. GIS was used to arrive at mapping units with uniform soil, slope percentage, slope length, land cover and land use to serve regional erosion study. The so-called SWEAP programme was used to calculate soil loss per land unit according to USLE and SLEMSA. Finally, the data on soil loss were translated in erosion hazard classes.

Résumé

Les interprétations des données du satellite TM et des photos aériennes sont d'importants outils pour la cartographie du sol. Ils permettent de planifier la surveillance du terrain en orientant les observations vers les sites les plus instructifs.

Le SIG permet un contrôle sur la valeur des unités d'interprétation des caractéristiques sélectionnées du terrain ainsi que la surveillance de la précision des limites des unités cartographiques en étudiant la relation entre l'information spectrale et les données spécifiques du terrain.

Il fournit aussi un instrument puissant qui est en mesure de faire des combinaisons utiles de données thématiques et d'en évaluer la valeur informative. Dans cette étude, des plans ont été établis sur les acquisitions de l'information, sur la cartographie du sol à l'échelle de reconnaissance et la cartographie des risques d'érosion dans une seconde phase en utilisant la télédétection, le SIG et dBase. Durant les recherches sur le terrain à l'échelle 1/30 000 de la seconde phase, l'accent a été mis sur l'élimination des lacunes dans l'observation du sol. Une carte d'utilisation des terres a été produite et des observations servant à constituer une base de données du terrain ont été faites suivant le système SOTER. Le SIG a été utilisé pour arriver aux unités cartographiques avec une uniformité en sol, pourcentage et longueur de la pente, couverture du sol et l'utilisation du terrain afin de servir aux études régionales sur l'érosion.

Le programme nommé SWEAP a été employé pour calculer la perte de terre par unité de terrain selon USLE and SLEMSA. Finalement, les données sur les pertes de terres ont été traduites dans la catégorie: risque d'érosion.

1. Introduction

The Kaya area (approx. 190 km²) is located north-east of the capital Ouagadougou in Burkina Faso (Fig. 1) between the coordinates 13°13'30"-13°6'0" N and 1°2'36"-1°6'48" W.

Geologically, the area consists of Precambrian schist, metavolcanites, migmatite and granite. In the Pleistocene, when relief of the schist landscape was more pronounced, plinthite was formed in soils of the piedmonts, which irreversibly hardened into ironstone. After intensive erosion of the schist hills and the piedmont zone, remnants of ironcaps generally form the highest components of the landscape.

The present ironcaps with footslopes are for reasons of high stoniness, low water holding capacity and high run off generally not used for annual cropping but for extensive grazing. Therefore, shrub vegetation and more or less permanent spots with stable herbs are present, leading to accumulation of aeolic material, which upon erosion by run off is transported downslope covering clay loams in broad valley land, containing valley bottoms (*bas fonds*) and adjacent pediments.

The analysis of drainage pattern identifies areas with high gully erosion in the valley bottoms. Normally, clay loams are exposed at these sites.

Gullied land and nearly abandoned badlands were found locally in the valley land of the study area. However, marks of sheet and rill erosion are found to be dominant features.

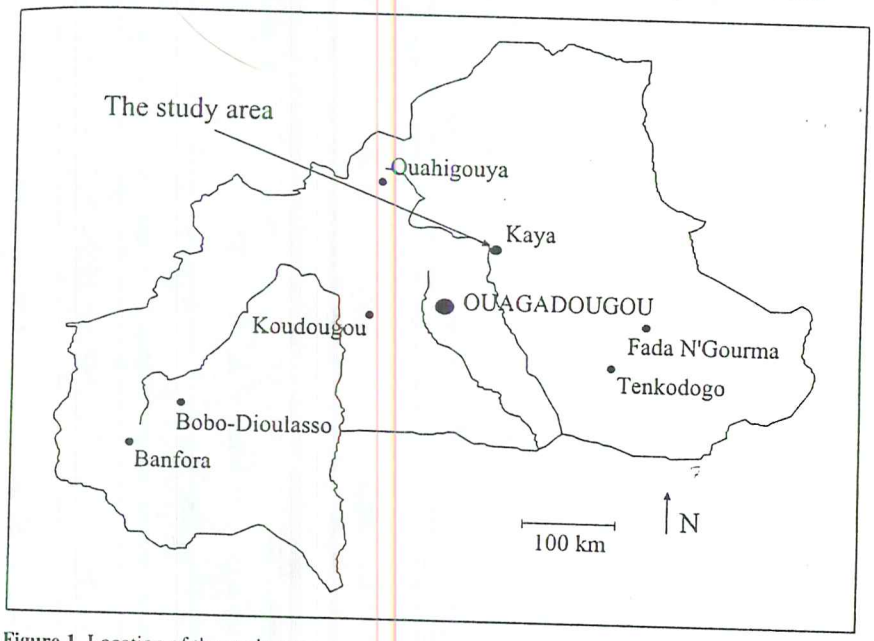

Figure 1. Location of the study area.

The variations in texture and soil depth are generally great in the valley land and the study area as a whole, which indicates different susceptibility to erosion of the soil units. In order to get insight in the erosion hazard of the soil units in the study area, soils as well as land use and land cover were identified.

The present research focuses on the application of remote sensing and GIS, using ILWIS (Integrated Land and Watershed management Information System: VALENZUELA, 1988) and erosion models to estimate erosion hazard in the study area with its specific terrain conditions. For this purpose, soil and terrain properties were described according to the SOTER system (World SOils and TERrain digital database: VAN ENGELEN and PULLES, 1991). The SWEAP (SOTER Water Erosion Assessment Program: VAN DEN BERG, 1992) programme was used to calculate soil loss according USLE (Universal Soil Loss Equation, WISCHMEIER and SMITH: 1978) and SLEMSA (Soil Loss Equation Model for Southern Africa: STOCKING *et al.*, 1988). The outcome of the erosion model calculations was used to estimate erosion hazard of the different mapping units.

2. Theoretical considerations on GIS

The present research is an example of information fusion. Several inputs belonging to different levels are combined. Each level has specific properties and requires its own quality measures and fusion technique (BARTL and PINZ, 1992). For instance, the level of aerial photo-interpretation may be combined with that of a classified satellite image. There are requirements for matching these levels and for fusion of information. For example, some mapping units may be identified by both levels. Others are not since level properties are different. Still information of both levels can be valuable for the research.

To enable coverage of two images, the image data of one image have to be made conform to the other (registration). Satellite imagery has a pixel by pixel registration, which by lack of sufficient topographic data may be the tool to be used for registration of other imagery. However if topographic data at suitable scale are available, the satellite image is georeferenced, that is map coordinates are assigned to the image data.

Information on aerial photographs has to be linked with that of topographic maps and/or satellite imagery by rectification: identical points are identified on both images and the software takes care of making both images conform in projection. For areas with high relief, appropriate techniques for correcting aerial displacement should be used.

The next steps are the location of observation points and mapping units as well as the study of thematic attributes.

In reconnaissance mapping, we identify complex terrain objects as aided by interpretation of remote sensing data and terrain observation. Observation points are registered of which the attributes are described in a separate database. The soil unit is an elementary object in an aggregation hierarchy as described by MOLENAAR and JANSSEN (1992), while the physiographic unit is a complex object.

The codes of mapping units on their turn may have a hierarchical structure: landscape - land unit - soil unit.

Since it concerns mapping at reconnaissance scale, the elementary object has a certain complexity, being often heterogeneous in soil conditions. At larger scales, the elementary object will generally be more homogeneous.

Other properties of the terrain, such as land cover, land use and vegetation, will be related to soil conditions in a variable way if human influence is high. Remote sensing is describing mainly surface characteristics of the earth surface (land cover etc.). Complete fusion with soil characteristics cannot be expected at high human impact.

Nevertheless, the information is of interest for environmental mapping. The link between remote sensing data, primarily in raster structure and GIS with object data in vector format can be done by identification of the raster elements (pixels): classification with the final aim of object identification (MOLENAAR and JANSSEN, 1992).

Classified remote sensing image data of one acquisition may be combined with remote sensing data of another acquisition or with image data of another information level by

crossing. The latter (e.g. by matrix) is a means to enable information fusion, that is combine information of different levels (e.g. soil and land use).

3. GIS applied in this research

The method applied in this research is illustrated in the flow chart of figure 2 (scheme modified from the example given by MOLENAAR and JANSSEN, 1992). The flow of information sources and acquisition, including control on accuracy and second fieldwork are indicated in this scheme. The TM image was georeferenced by GPS data.

The main GIS activities were in the fields of referencing aerial photographs with TM imagery and crossing of map data. Data modelling and classification were final activities.

4. Reconnaissance soil mapping

The study area was mapped at a scale of 1:30,000 aided by TM satellite data (acquisition: January 8, 1991), enlargements of aerial photographs with original scale 1:50,000 (acquisition: January, 1982) and aerial photographs of scale 1:30,000 (acquisition: October 1981).

The method used for soil mapping is illustrated in table 1. Five stages are recognized. The innovative methods are presented in bold characters. For physiognomy used as a basis for description of soil surface and other terrain properties, the reader is referred to POUGET and MULDERS (1988).

Table 1. Reconnaissance soil mapping.

	Stage	Method	Results
I	Pre-fieldwork	SII (Satellite Image Interpretation) API (Air Phot-Interpretation)	First appraisal of land cover Physiographic units and drainage pattern.
II	First fieldwork	Landscape guided soil and terrain observation Physiognomy, field reflectance, dBase	Land description, soil data, location of observations on APs Reflectance data, terrain database.
III	Digital data processing	SAD* classification, georeferencing and rectification, APs-TOP**-SAD	Prel. land cover map, observations map, roads map, drainage systems map, physiographic map, preliminary soil map.
		Crossing of prel. soil map with SI	Control on boundaries of mapping units.
		Queries to terrain database + API	Sites to investigate in final fieldwork.
IV	Final foeldwork	Soil and terrain observation at sites/outcome III, dBase	Completion of terrain database
V	Final digital data processing and interpretation	Queries to terrain database, API, SII and classification	Final legends, final maps on land cover, land use and soil.

* SAD : SAtellite Data; **TOP : TOPographic data.

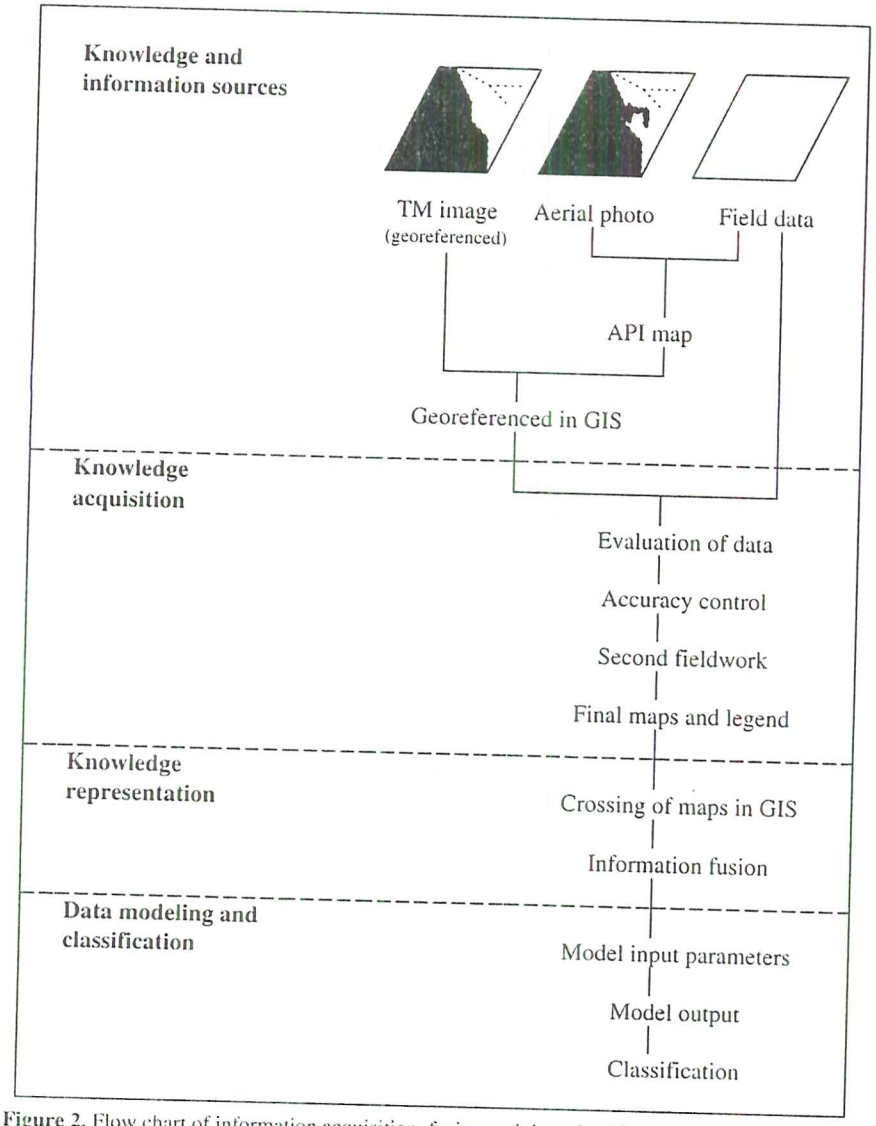

Figure 2. Flow chart of information acquisition, fusion and data classification.

The physiognomic description is used with field reflectance data to get understanding of the multispectral reflectance of land cover. Modelling has to be used to arrive from detailed measurement at land components to land cover data, which can be correlated with low resolution remote sensing data (MULDERS *et al.*, 1992).

For satellite image interpretation and crossing of preliminary soil map with the satellite image, the reader is referred to MULDERS and CASTERAD (1996).

The repeated interaction of interpretation maps with the terrain database to control boundaries and improve accuracy cannot be emphasized too much. Besides digitizing map and image data, it is the most outstanding aspect of the proposed method. Also dBase actions to produce the final legend belong to this category.

5. Erosion hazard mapping

The method applied for erosion hazard mapping in this research is based on characterizing soil units by SOTER properties and subsequent application of SWEAP software to calculate soil loss according to the USLE and SLEMSA erosion models.

The SOTER methodology, normally applied at exploratory scale, is used in this research to characterize soil units at reconnaissance 1:30,000 scale.

The method is schematically represented in Table 2. In this table, c- and f-values are mentioned.

The c-value is the cover and management factor in USLE. The factor is 0 for complete protection of soil and 1 for a clean-tilled fallow. Since it concerns multiple land use types with permanent or shifting cultivation and grazing, a physiognomic appraisal of % of trees, grass + herbs and crops per land use type produced the best results, using c-factors according to KASSAM (1991; results on c-factor estimations are given in MULDERS, 1995).

The f-value stands for the SLEMSA intrinsic soil erodibility in dependence of soil texture class and type of soil development (VAN DEN BERG, 1992).

Interpretation of TM satellite imagery (NDVI or Normalized Difference Vegetation Index) was used for estimation of density of land cover. The resulting land cover map was crossed with the land use map to produce land use units with classified vegetation cover: LUCO in Table 2.

To arrive at soil units with specified land use and vegetation cover, the soil map was crossed with the LUCO map: LUCOSO in Table 2. Queries to the terrain database and statistical calculations in dBase were the tools to define the average characteristics per unit. However, the estimation of slope length needed a specific approach as detailed below.

The characteristic slope length, needed for SOTER formulation (phase IV, Table 2), was difficult to estimate by lack of field data on slope direction. However, GIS may help, also in this case. The ILWIS system enables processing a distance map, representing isodistance lines as determined by the distance to nearest drainage ways (Fig. 3).

The distance map was crossed with the LUCOSO map. Each unit of the LUCOSO map could be characterized by pixel frequency and distance measures (Fig. 4: example).

In figure 4, unit A312 representing (very) gently sloping glacis (valley land), is partly adjacent to the drainage way (0-150 m). However, different populations are found around 175 m and 320 m distance from the drainage way.

The graphs appeared to represent complex units. It was necessary to simulate different forms of the LUCOSO map and estimate formulae to determine average slope length per unit. Some of the simulated forms are given in figure 5.

Table 2. Reconnaissance erosion hazard mapping acc. SOTER and SWEAP.

	Stage	Method	Results
I	Pre-fieldwork	Interpretation land cover, land use and soil maps	First appraisal of eroded areas
II	Fieldwork	API and SII Observation of SOTER characteristics, dBase API, SII and terrain observation	Selection of observation sites. Field characteristics SOTER database. Details on erosion and accumulation. Land cover.
III	Laboratory analyses	Analyses of topsoil samples.	Texture, EC and OM.
IV	Digital data processing	Crossing land use and land cover maps.	LUCO combination.
		Crossing LUCO with soil map. Queries to terrain database.	LUCOSO combination. Legend terrain, soil and land cover LUCOSO units.
V	Application of SWEAP	Produce distance map. Crossing of LUCOSO with distance map. SOTER data file.	Distance of drainage ways. Slope length (SLEN). Completion of SOTER database incl. III and SLEN.
		TAB files.	Climatic data, land use and vegetation (c- and f- values).
		Run the models. Classification soil loss.	Soil loss and factors USLE and SLEMSA. Erosion hazard rating.

Neglecting the d = 0 value, the graph in figure 4 is thought to be built on GD from d = 0-100, RO from d = 100-280 and GD from d = 280-500. Based on the simulated forms of figure 5, approximations of formulae to calculate the slope length, or the length of unit as measured from the drainage way, were made, using y-x d-values, average frequencies and weighted average d-values of segments in case of complex curves, such as that from figure 4. Attention should be paid to hills with opposite slope directions and different distances to drainage ways from one direction and others, which lead to errors in estimation of slope length.

The resulting slope length data per LUCOSO unit were registered to complete the SOTER file. The TAB files with data on climate, land use and vegetation were compiled to run SWEAP, the programme compiled to calculate soil loss according to USLE and SLEMSA.

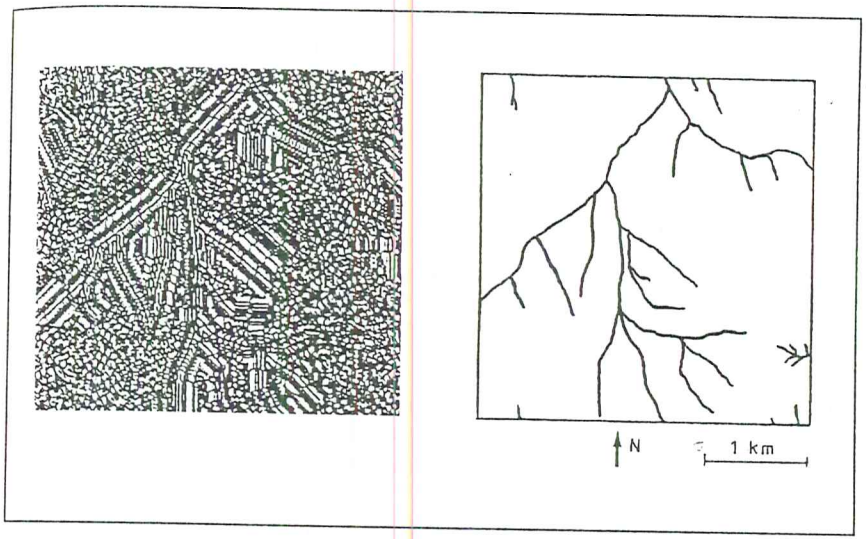

Figure 3. ILWIS/iso-distance (left) and drainage pattern (right) of central part of the Kaya Region.

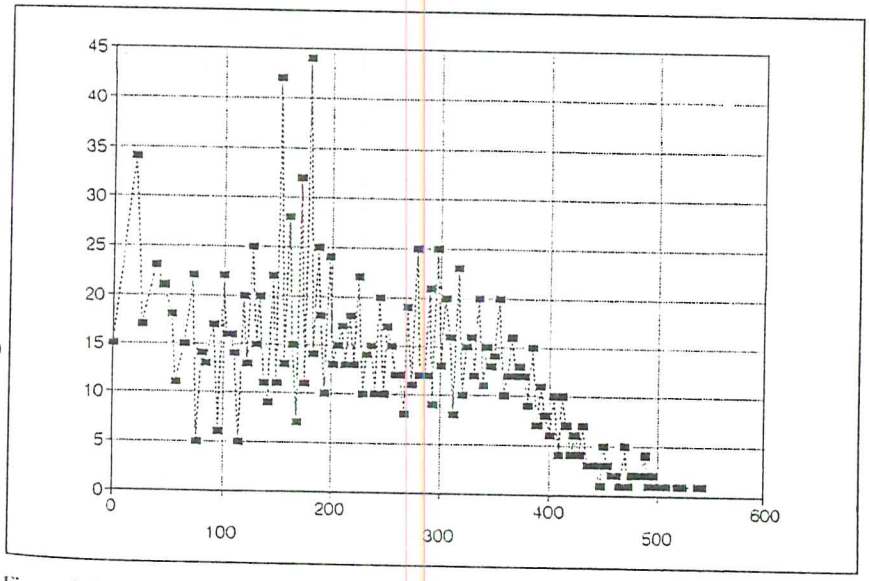

Figure 4. Graph of frequency (y-axis) and distance of drainage ways (x-axis) of unit A312 with AV, produced by QPRO.

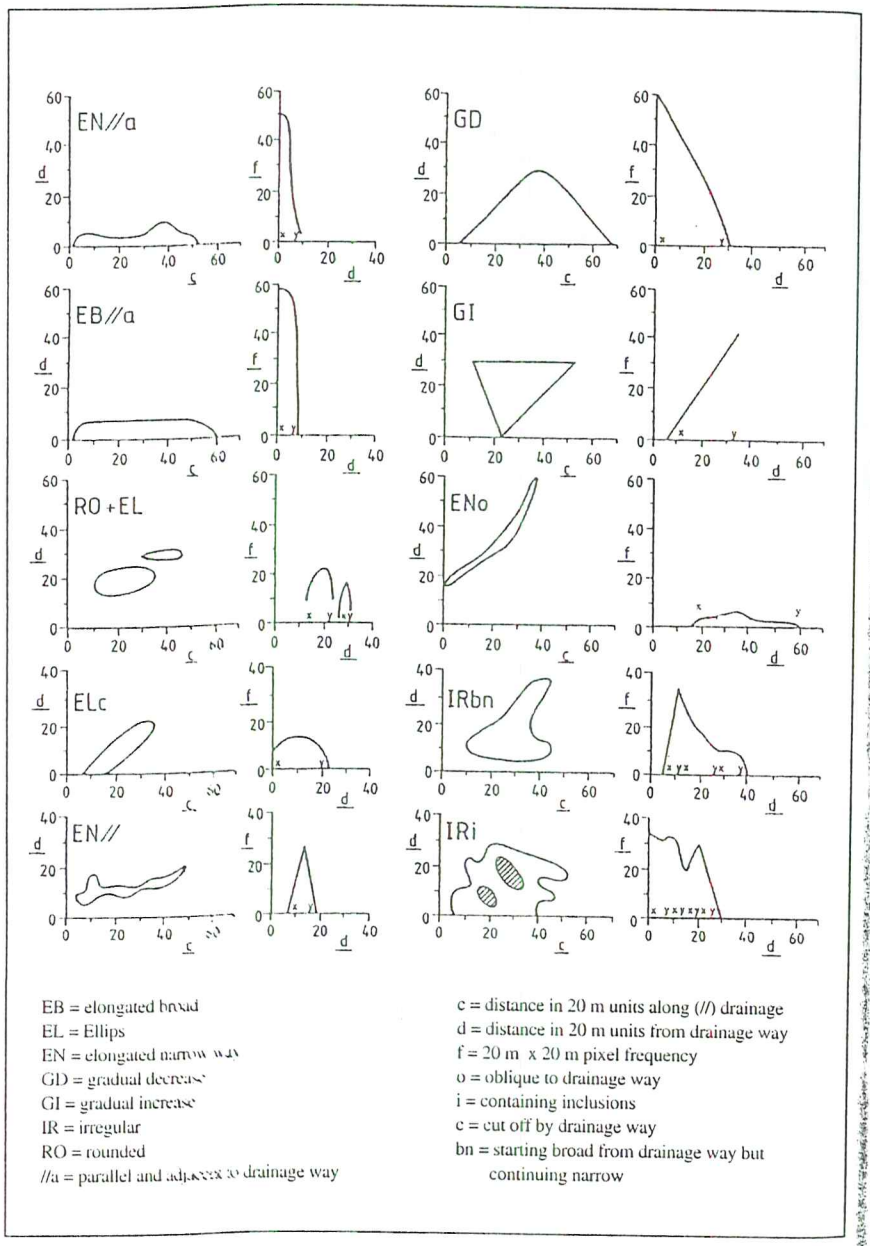

Figure 5. Simulated forms for distance appraisal of mapping units.

6. Results

The area was subdivided into the following landscape and soil units (between brackets: soil classification according FAO-UNESCO, (1994 and CPCS, 1967):

A. Landscape with schist and meta-volcanites.
- A1. Soils of the hills (Lithosol, Eutric Regosol, *Sol brun eutrophe tropical*).
- A2. Soils of the ironcaps (Lithosol, *Sols minéraux bruts d'apport éolien*, *Sols peu évolués lithiques et régosoliques*).
- A3. Soils of the valleys (Eutric Fluvisol, *Sol peu évolué d'apport alluvial*).
- A4. Rock outcrops.

B. Landscape with granite and migmatite
- B1. Soils of the ironcaps (see A2).
- B2. Soils of the valleys (Dystric Regosol, *Sols minéraux bruts d'apport alluvial*; Eutric Fluvisol, *Sol peu évolué d'apport alluvial*).
- B3. Rock outcrops.

The results on soil loss data of LUCOSO units, each covering more than 2% of the study area, are given in Table 3. For description of soil units as outcome of dBase (Table 4).

Soil loss calculated according SLEMSA appeared to be always higher than calculated according USLE. To illustrate soil distribution, land use and erosion hazard, those maps are given of the central part of the area in figure 6. For description of land use units, see Table 5.

Table 3. Soil loss according USLE and SLEMSA and erosion hazard classification.

LUCOSO (Unit nr.)	Area (%)	Soil (Code)	Land use (Code*)	Soil loss (tons/ha/yr) USLE	SLEMSA	Erosion hazard USLE
8	5.7	A150	CB	4.9	12.8	3
9	2.6	A150	CBH	1.3	3.4	1
12	2.0	A150	PH	0.8	2.1	1
23	4.0	A240	P	5.8	19.6	3
25	4.3	A312	AV	4.2	18.2	3
37	2.6	A340	AV	4.1	16.0	3
45	2.8	B121	CV	2.7	5.0	2
57	2.4	B140	P	4.2	23.6	3
61	6.8	B211	AV	7.0	17.7	3
67	8.5	B213	AV	9.3	26.7	3
75	4.0	B230	AV	10.4	18.9	4
79	2.4	B230	CV	8.6	15.6	3

* For explanation of codes: see Table 5.

7. Discussion

The maps in figure 6 illustrate the pattern of erosion hazard. There is some resemblance of erosion hazard with the soil map, but it is more the combination of soil and land use with the specific SOTER characteristics, such as slope length, soil structure and texture of the topsoil, which determine the erosion hazard class. Due to the classification of erosion hazard, there is a general simplification, especially in the landscape with granite and migmatite (B).

Table 4. Description of soil mapping units of study area (Fig. 6).

Code	%	Average slope	Surface gravel	Surface blocks	Drainage cond.*	Depth (cm)	Texture 0-30 **	Texture 30-60	Texture 60-120
A130	100	4.5	44	27	W	27	cl		
A150	87	2.1	48	5	W	31	sl	l	
	7	11.0	32	8	I	19	sil/c		
	6	3.0	18	10	I	94	sl	scl	scl
A210	100	3.6	37	6	R	10	sl		
A222	54	2.0	27	7	W	78	sl	cl	cl
	46	2.1	27	7	R	10	sl		
A230	100	18.3	39	12	R	10	scl		
A240	100	3.6	26	9	W	39	scl	scl	
A312	93	1.9	19	8	W	32	scl	scl	
A313	100	3.0	2	1	R	85	ls	ls	ls
A314	82	1.6	13	4	W	48	sl	scl	
	18	2.8	25	7	W	25	ls		
A330	100	1.3	14	9	W	63	scl	cl	c
A340	100	1.3	25	4	W	75	scl	scl	cl
B110	100	2.0	50	15	R	10	sl		
B121	100	2.0	45	12	R	29	sl		
B122	78	3.4	43	7	R	19	sl		
	22	3.0	15	8	W	100	sl	sl	sl
B130	100	32.0	58	28	R	11	scl		
B140	100	4.5	26	21	W	41	ls	sl	
B211	84	2.0	21	5	W	37	sl	sl	
	9	1.7	7	1	W	99	sl	sl	sl
	7	2.8	55	10	R	2	sl		
B213	92	2.0	8	3	W	98	ls	sl	sl
B230	91	1.3	8	2	I	95	sl	l	cl

* Drainage condition: rapidly (R), well(W), imperfectly(I); ** Soil texture: silty(si), sandy (s), loam / loamy (l), clay (c).

The classification of erosion hazard applied in this study needs further elaboration.

However, the main aim of the study was to test GIS and Remote Sensing for estimation of erosion hazard. GIS, used for combination of soil and land use as well as combination with land cover, appeared to be an essential tool. An interesting application of GIS is the estimation of slope length by isodistance lines from the drainage ways. At the moment, that

was the goal. However, the present visual interpretation of graphs should be replaced by geostatistical methods to calculate slope length. Moreover, the average distance of mapping units to the drainage way itself may be used in models to calculate runoff contribution from more distant units to those more near to the drainage way.

It has to be taken in mind, that the SOTER system was compiled for small scale mapping. Estimation of land use and vegetation was found to be difficult according to the classification and model input data given in the manual. Adaptations were necessary to apply the system at scale 1:30,000. It is advisable to take physiognomic vegetation properties as an entry to classification of land use and vegetation.

Database management and SWEAP were appropriate to carry out the soil loss calculations. The present appraisal is a per unit calculation of soil loss for average rainfall conditions; the influence of runoff coming from units upslope is not accounted for.

Table 5. Description of land use units (Fig. 6c).

Code	Description	Trees	Shrubs	Grass	Agric. fields	Bare land
P	Pasture (*pâturage*)	3	7	14	38	76
CV	Intensively cultivated high fertilization level (*champs de village*)	4	5	6	60	85
CB	Extensively cultivated (*champs de brousse*)	6	7	13	46	75
AV	Valley bottom with fruit trees	9	7	10	40	75

If we compare the results on soil loss and erosion hazard with those derived for exploratory scale by OLDEMAN *et al.* (1991), the degree of degradation estimated by these authors seems to be exaggerated. The area north of Ouagadougou was characterized by the following indication: Wt3.5/Wd3.3 g/a, where Wt stands for loss of topsoil and 3.5 for strong degree of degradation (50-100% of the area affected); Wd is indicating terrain deformation/mass movement, 3.3 is strong degradation (10-25% of the area affected), g/a indicates the cause by overgrazing/agricultural activities. At small scale, we would prefer to go one step back in degree of degradation.

Conclusions

The application of GIS and remote sensing together with dBase, is promising for assessment of erosion hazard. Remote sensing with multispectral satellite data was useful for soil survey and for estimation of density of land cover.

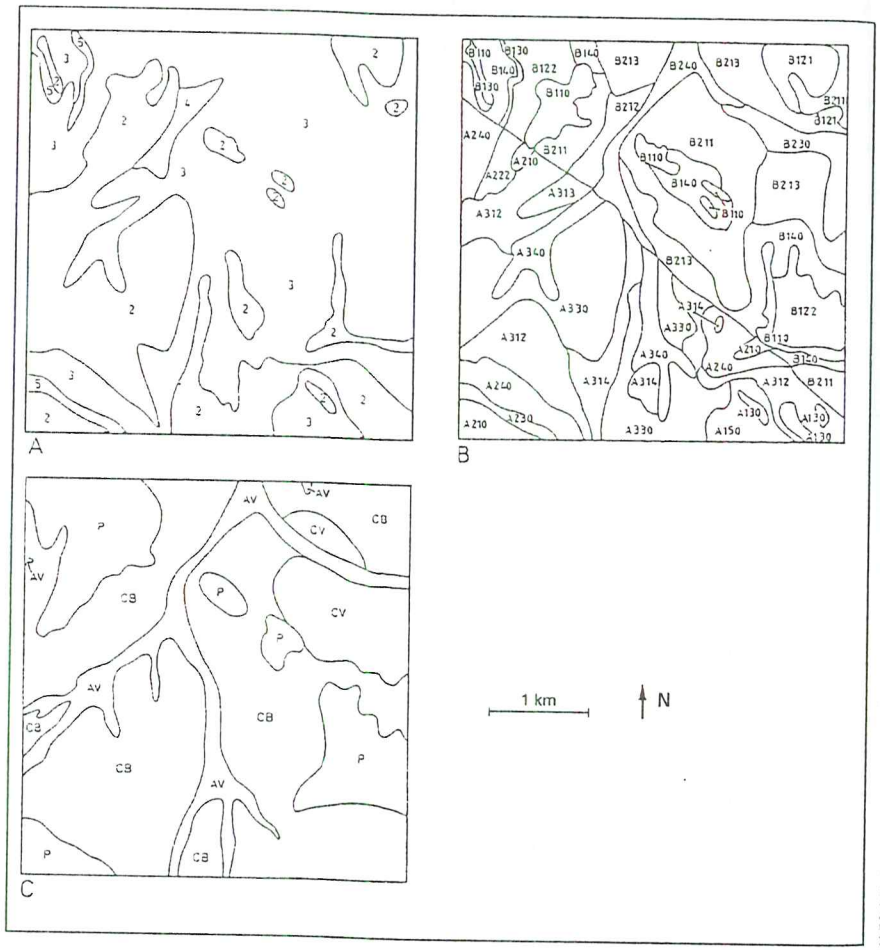

Figure 6. Erosion hazard (A), soils (B) and land use (C) in central part of the study area.
Erosion hazard classes (USLE): 0: < 0.3; 1: 0.3-1.5; 2: 1.5-4; 3: 4-10;
(tons/ha/yr) 4: 10-20; 5: 20-50; 6: 50-150; 7: > 150.

Slope length estimation using isodistance from the drainage ways and moreover the average distance from the drainage way per mapping unit are aspects, which have to be further studied to improve erosion hazard estimation. For example, the models should include the contribution of runoff from upslope units for erosion hazard estimation.

The medium scale approach was useful to test the validity of exploratory scale assumptions on SOTER characteristics. The study of key areas will improve the exploratory scale surveys on degradation.

References

BARTL R., PINZ A. (1992). "Information Fusion in Remote Sensing: Land Use Classification". *Proc. of the Int. Workshop IAPR TC7*, Delft, The Netherlands: 9-17.

CPCS (AUBERT, BOULAINE *et al.*) (1967). Classification des Sols. Comm. de Pédologie et de Cartographie des Sols, INRA: 96.

FAO-UNESCO (1994). Soil Map of the World. Revised Legend with corrections. Technical Paper 20, ISRIC, Wageningen, The Netherlands: 140.

KASSAM A.H., VAN VELDHUIZEN H.T., MITCHELL A.J.B., FIS and AHAH M.M. (1991). "Agroecological land resources assessment for agricultural development planning. A case study of Kenya. Resources database and land productivity." Technical Annex 2, *Soil Erosion and Productivity*, FAO/IIASA: 54.

MOLENAAR M., JANSSEN L.L.F. (1992). "Terrain objects, their dynamics and the integrated processing of remote sensing data". *Proc. of the Int. Workshop IAPR TC7*, Delft, The Netherlands: 113-134.

MULDERS M.A., DEN DULK J.A., UYLENHOET R. (1992). "Description of land surfaces, reflectance measurements and modelling for correlation with remote sensing data". *Science du Sol*, Vol. 30, 3: 169-184.

MULDERS M.A. (1995). "Inventory of soil, land use and erosion hazard at medium scale in the Kaya region". Document de Projet n°30, SPS/WAU: 50.

MULDERS M.A., CASTERAD A., (1996). "Preliminary results of processing terrain and remote sensing data of the Zablou area (Burkina Faso)". *Proc. 6th Symposium of the ISSS Working Group Remote Sensing (WGRS)* in cooperation with WGDM and WCASS, Ouagadougou, Burkina Faso.

OLDEMAN L.R., HAKKELING R.T.A., SOMBROEK W.G. (1991). "World map of the status of human-induced soil degradation. An explanatory note". Winand Staring Centre, ISSS, FAO, ITC-Enschede, The Netherlands: 34.

POUGET M., MULDERS M.A. (1988). "Description of the landsurface for correlation with remote sensing dat". *Proc. of 5th Symposium of the ISSS Working Group Remote Sensing*, Budapest, Hungary: 153-158.

STOCKING M.A., CHAKELA Q., ELWELL H.A. (1988). "An improved method for erosion hazard mapping". Part I: The Technique. *Geografiska Annaler*, 70 A.3: 169-180.

VALENZUELA C.R. (1988). ILWIS overview. ITC Journal 1988, Vol. 1, Enschede, The Netherlands: 4-44.

VAN DEN BERG M. (1992). SWEAP. "A computer program for water erosion assessment applied to SOTER (version 1.4)". International Soil Reference and Information Centre, ISRIC, SOTER Report 7 (ISRIC and UNEP), Wageningen, The Netherlands: 27.

VAN ENGELEN V.W.P., PULLES J.H.M. (1991). "The SOTER manual. Procedures for small scale digital map and database compilation of soil and terrain conditions". 4th Edition, Working paper and Preprint 91/3, International Soil reference and Information Centre, ISRIC, Wageningen, The Netherlands: 92.

WISCHMEIER W.H., SMITH D.D. (1978). "Predicting rainfall erosion losses - a guide to conservation planning". US Dept.of Agric., Agric. Handbook No 537: 58.

Preliminary Results of Processing Terrain and Remote Sensing Data of the Zablou Area (Burkina Faso)

M.A. MULDERS [1], A. CASTERAD [2]

1. Wageningen Agricultural University, Soil Science and Geology, POB 37 - 6700 AA Wageningen, The Netherlands.
2. Diputaciòn General de Aragon, Servicio de Investigaciòn Agraria, Unidad de Suelos y Riegos, POB 727, 50080 Zaragoza, Spain.

Abstract

Interpretation products of aerial photographs and satellite imagery were used in IDRISI together with information on terrain data in a dBase file to evaluate information obtained during a first field reconnaissance. GIS enabled to study a complex soil attribute and multispectral satellite data in relation to physiographic soil boundaries. Consequent aerial photo-interpretation and digitizing on screen produces imagery with indication of areas to be checked in a final fieldwork.

Résumé

Les résultats de l'interprétation des photos aériennes et des images satellitaires ont été utilisés dans IDRISI conjointement avec un fichier dBase contenant les données du terrain pour évaluer l'information obtenue lors de la première reconnaissance du terrain. Le SIG permet d'étudier l'ensemble des caractéristiques du sol ainsi que les données multispectrales du satellite en relation avec les limites physiographiques du sol. Par la suite, l'interprétation des photos aériennes et la digitalisation des images sur écran, reproduit des nouvelles images avec l'indication des régions qui doivent être examinées durant la recherche finale sur le terrain.

1. Introduction

The Zablou area is located north-west of Kaya along the road from Kaya to Lac Dem (Fig. 1). The area served as a test area for application of techniques to produce maps from results of airphoto-interpretation, satellite data and terrain data.

Three programs were used (CASTERAD, 1992) :
- GEO-PAKKET to digitize maps of airphoto-interpretation,
- ERDAS 7.4 to process satellite data,
- IDRISI 4.01 to combine data of remote sensing, airphoto-interpretation and terrain.

At the start of the research, the following data were available:
- remote sensing imagery,
- a first interpretation of landscape, physiography and soils,
- a terrain database as result of a first fieldwork.

The research aims to answer the question: "Do GIS and remote sensing techniques help in evaluating interpretations on physiography and soils after a first field reconnaissance ?"

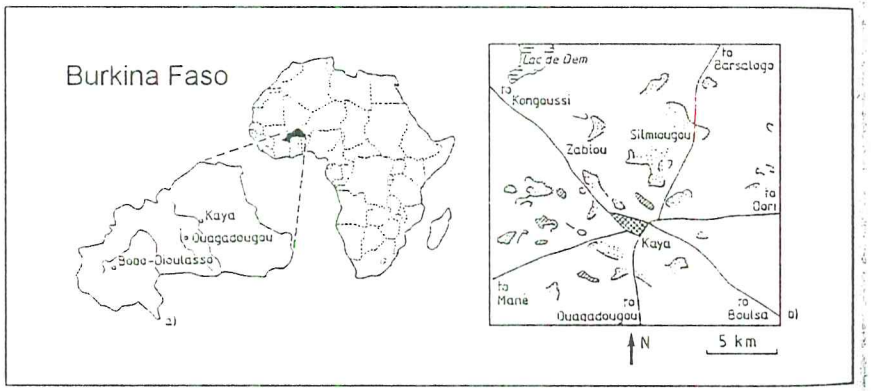

Figure 1. Location of the Zablou study area.

2. Results of first field reconnaissance

The landscape of the Zablou study area was subdivided into four units :
- A: high steeply dissected land with ironcaps;
- B: moderately high plateauland with ironcaps;
- C: land with elongated hills as dominant features;
- D: valley bottom land.

The landscape units were subdivided into physiographic components according to position and slope. Coding of the units and their components according to their relative elevation from high too low, enabled orthographic display by the ORTHO programme in IDRISI (EASTMAN, 1992). Plate 3a presents a view towards the north-east.

A terrain database was developed in dBase IV, showing columns per row, or observation number, with data on:
- x and y coordinates;
- physiography a.o. slope %;
- soil code indicating, respectively soil depth, surface stoniness, soil texture and profile development;
- surface stoniness (%), crusted surface (%), gravel at surface (%);
- soil texture and coarse fragments with 20 cm interval;
- matrix colour with 20 cm interval; if colour is registered according hue, value and chroma in separate columns, calculations are possible;
- 1st and 2nd dominant colour of mottles;
- type and depth of blockage in cm;
- % of area with sheet and rill erosion;
- % of coverage by trees, shrubs, grass and herbs;
- % of coverage by agricultural fields;
- % of coverage by millet, sorghum or by other crops;
- % of coverage by bare soil;
- % of coverage by rock outcrops (+ type);
- height (cm) and % of coverage by dunes;
- length of stone dikes m/3600 m².

3. Results of processing after the first fieldwork

Digitizing the information represented on aerial photographs was done according to GEO-PAKKET, software developed by the Dept. of Landsurveying and Remote Sensing and the Centre for Geographic Information processing (Wageningen Agricultural University) to correct for radial distortion on aerial photographs in digitizing.

Since there were no other topographic data available than those at scale 1:200,000, a Landsat TM (Thematic Mapper) image (acquisition 8th January 1991), corrected by GPS data, was used as base map (reference map). For registration, identical points had to be identified on the TM image and the aerial photograph. This was done in the ERDAS programme (ERDAS, 1991).

Resulting digitized maps were those on physiography and observation points.

Part of the map on physiography (with 14 units) is shown in plate 3b. The units reproduced in plate 3b are the following:
- *chs* or remnants of high ironcaps (5);
- *che* or eroded high ironcaps (3 + 13);

- *cpr* or steep slopes of high ironcaps (12);
- *l* or elongated hills with steep slopes (2);
- *n* or relatively low hills (14);
- *bpw* or footslopes with colluvial material (4);
- *bpv* or footslopes with fluviatile deposits derived from aeolic and colluvial materials (10);
- *pfd* or faintly sloping area with weak erosion (8);
- *p'fg* or faintly sloping and sloping areas with moderate erosion (1);
- *pfd* or faintly sloping areas with moderate erosion (11);
- eroded low ironcaps (6);
- *cbs* or remnants of low ironcaps (9);
- *ak* or valley bottoms (7).

ERDAS was used to produce different TM images for interpretation. After translation of ERDAS format into IDRISI format, IDRISI enables easy coverage of remote sensing and GIS imagery, that is by simple key operation. An example (colour print) is given in plate 4.

4. Image interpretation

The time of acquisition of TM data was at the start of the dry season. Valley bottoms contained at that time green vegetation at many places, as witnessed by reddish tones (Plate 4).

The footslopes at the foot of the ironcaps in the northern part of the area are pictured on this figure in white tones, being sandy soil surfaces with scarce vegetation.

The ironcapped plateaux are represented in dark tones, having low reflection in all bands of the combination. There is no difference in tone between the elongated hills of landscape C and the ironcaps of landscape B. These units, however, could be discriminated by a combination of the first three principal components (PC 1-2-3) of the same TM acquisition. For general principles on satellite image interpretation, the reader is referred to MULDERS (1987).

Possibilities of interpretation are highly influenced by image production. In this research, the Canon laser printer CLC 300 was compared with the Tektronix 4693dDX. The latter has a dotty character and enables direct printing of ERDAS imagery with reasonable detail in dark tone areas like ironcaps. The former is able to produce high quality imagery if properly treated in ARC/INFO.

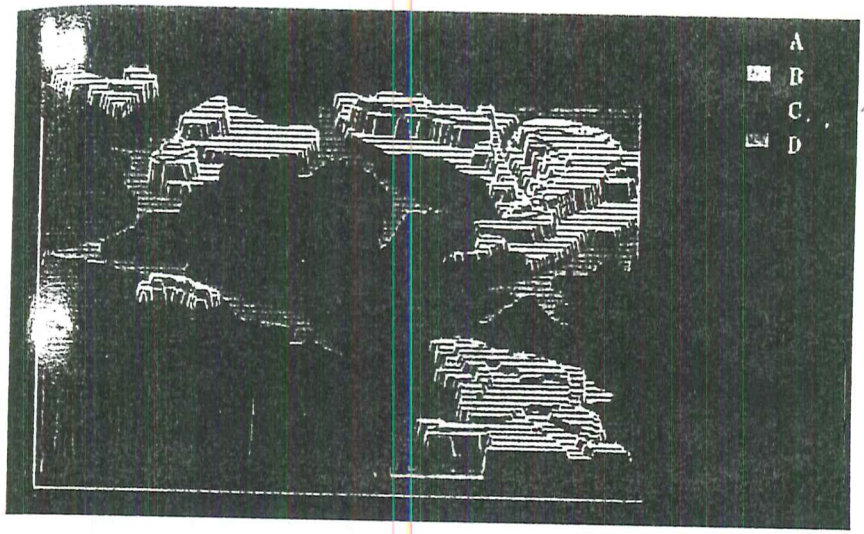

Plate 3a. Ortho-view towards the north-east of the Zablou area in Burkina Faso (p. 197).

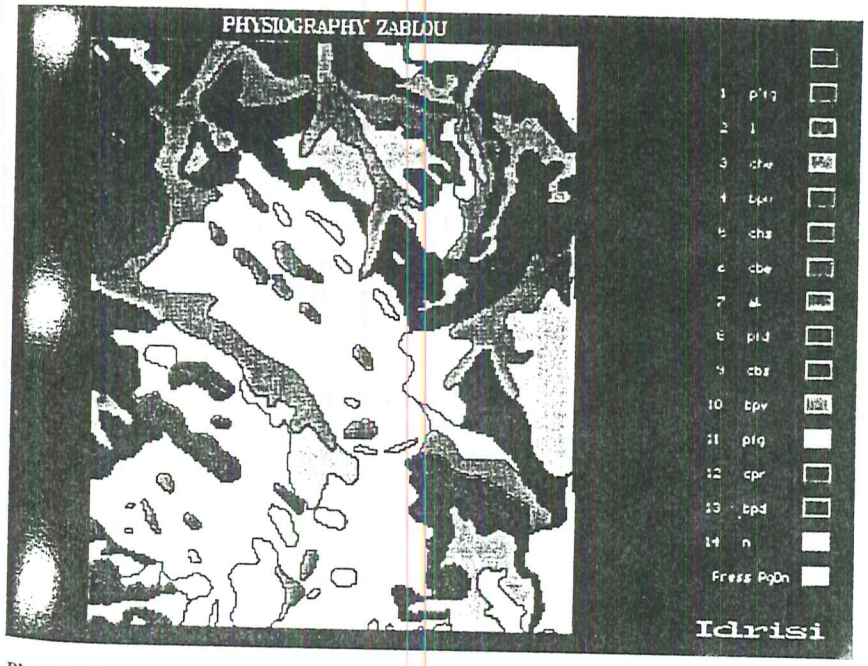

Plate 3b. Physiographic map, showing 14 units of the Zablou area, Burkina Faso (p. 197).

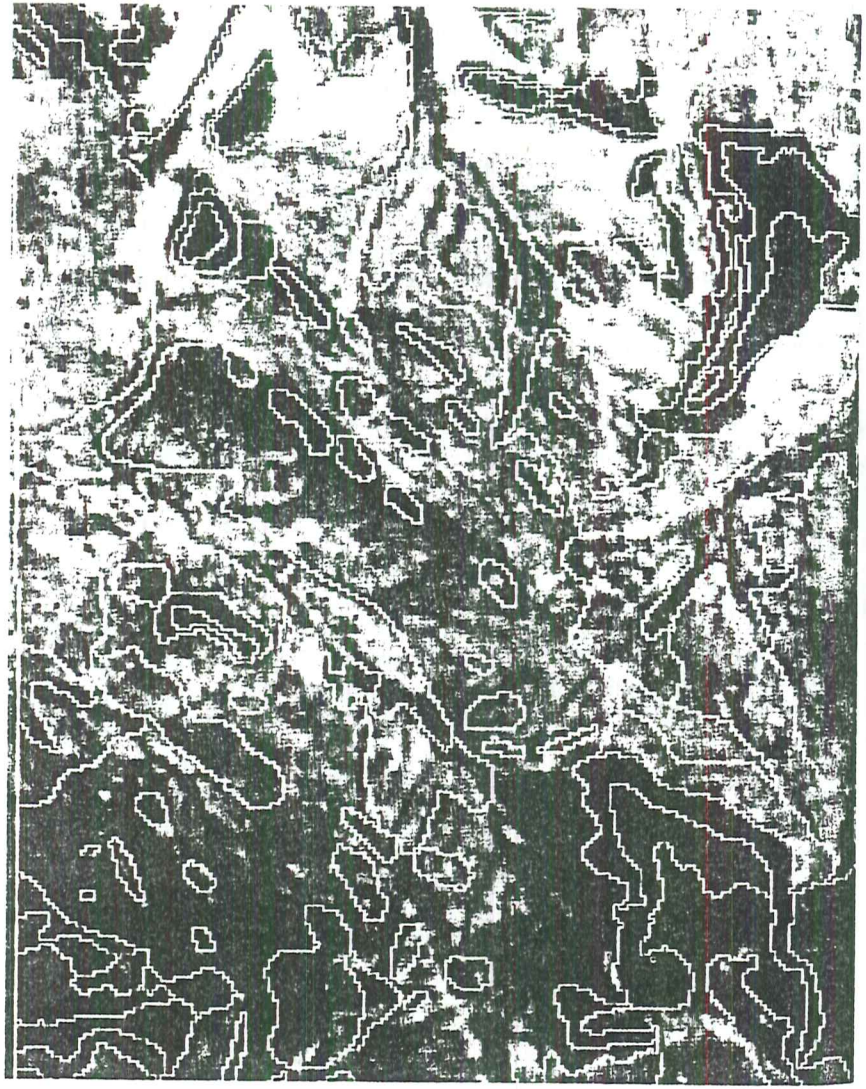

Plate 4. Landsat TM 4-5-3 image of 8 January 1991 overlain by a map on physiography, Zablou area, Burkina Faso (p. 198).

5. Combination of terrain data with remote sensing and GIS data

IDRISI 4.01 enables to combine one attribute per observation point with identifiers (x and y coordinates). For creating a highly informative complex attribute, the soil depth and soil texture columns were checked for the following:

Code:	Check for:
1	Blockage <= 30 cm;
2	Horizons with clayey texture in profiles deeper than 60 cm;
3	Loam, loamy sand, sandy loam or clay loam in 0-40 cm or 0-60 cm.

The result for a small part of the image of plate 4 is given in Fig. 2.

In IDRISI, the data of figure 2 were superimposed on the TM 453 image (Plate 4) enabling the checking of boundaries by the complex soil attribute and by the multispectral information of the TM image. The latter provides for a means to control boundaries if relationships with terrain properties are understood.

For example, a dark tone on the hill units may be related to the exposure of bare rock. Checking the TM image with physiographic boundaries proves that the same multispectral signature is present on part of the footslope area. Interpretation of aerial photographs demonstrates bare rock to be likely in those parts. It was missed in interpretation because physiography was based on analysis of site (position in toposequence) and slope. Apparently, the footslope has to be divided in more than one unit as it first became apparent by multispectral analysis.

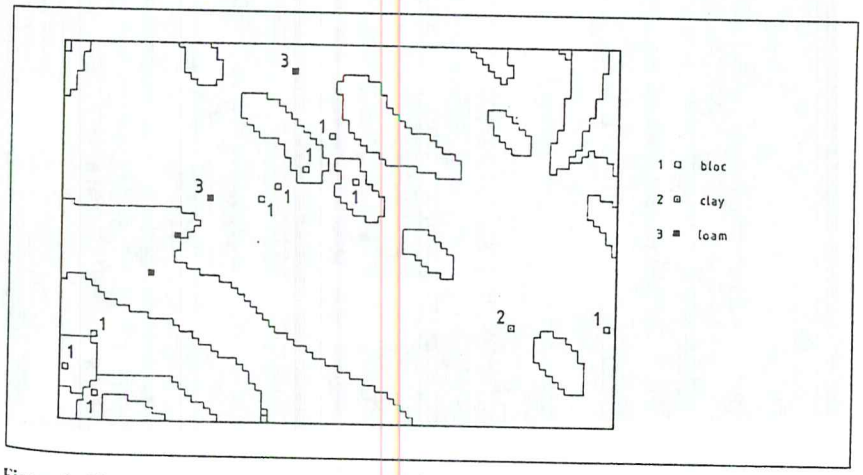

Figure 2. Observation points with code of complex attribute projected on physiography.

Another possible application of multispectral capability for this purpose is found in the magenta-red colours of plate 4. These colours indicate relatively abundant vegetation cover,

which often point towards relatively deep soils. However, exceptions exist on this rule since protection measures may be the underlying cause of abundance of vegetation.

A plan for field check in the second fieldwork phase can be made as based on this and other evidence of comparison between multispectral data and interpretation of aerial photographs. An image can be made in IDRISI showing a remote sensing image at background, covered by physiographic soil boundaries and showing the areas to be checked during the second fieldwork in different colours.

Conclusions

The combination of terrain data with remote sensing data in GIS is promising to direct field observations in the second phase of fieldwork to those places, where observations are most likely to be effective for improving accuracy and for raising the informative value.

Five phases can be recognized in the approach to soil mapping using modern techniques besides the conventional ones, these being:

- pre-fieldwork with processing satellite data and interpretation of aerial photographs;
- first fieldwork with terrain observations guided by the interpretation products and production of a terrain database;
- digitizing of the interpretation maps and GIS for control of boundaries between mapping units with the aid of the information contained in the terrain database to construct a plan for fieldcheck in the final fieldwork phase;
- final fieldwork to complete terrain observations and database;
- final digital data processing and interpretation.

It is worthwhile to pay much effort into understanding the relationships between remote sensing data and actual terrain conditions in key areas with the purpose to speed up mapping of adjacent areas.

References

CASTERAD A. (1992). "Processing and analysis of remote sensing and terrain data for agricultural management in arid conditions", Final report EC grant ref. ST920238 : 14.

EASTMAN J.R. (1992). *User's guide IDRISI version 4.0*, Clark University, Massachusetts, USA:178

ERDAS (1991). *ERDAS field guide*. Second edition, Version 7.5./ ERDAS Inc, Atlanta USA: 394.

MULDERS M.A. (1987). *Remote Sensing in Soil Science*. Developments in Soil Science 15, Elsevier, Amsterdam: 379.

Deriving Sub-Pixel Soil Characteristics in Northern Burkina Faso with Spectral Unmixing

Maarten TROMP, Marcel Z. STEENIS

Department of Soil Science and Geology, Wageningen Agricultural University
P.O. Box 37, 6700 AA Wageningen, The Netherlands
E-mail: maarten.tromp@algemeen.beng.wau.nl

Abstract

In this paper the possibilities and advantages of spectral unmixing for information extraction of Landsat TM data are analysed. Raw image data are transferred to field reflectance data with the empirical line method. "Harmattan dust" blown from the Chad basin to the Sahel during the dry periods had, although not visible on hardcopies, a large influence on the reflected radiance represented by the Landsat TM image of May 7, 1988. Resampled field reflectance spectra could be used for the spectral unmixing of Landsat TM. The results of the spectral unmixing resembled the field estimations closely. Units of research showed a tendency of increased coverage with dead grass at the expense of sand in the period between the date of image acquisition and the fieldwork. This corresponded with the presence of deserted agricultural fields due to decreased fertility after intensive agricultural use.

Résumé

Ce rapport fait l'analyse des possibilités et des avantages de la méthode de déconvolution spectrale pour l'interprétation des images Landsat TM. Les données brutes de l'image sont transformées en valeurs de réflectance de terrain par la méthode de la ligne empirique. Sans que cela soit visible sur les *hardcopies*, la poussière d'harmattan emportée du bassin du Tchad au Sahel par le vent pendant les périodes sèches avait une grande influence sur la radiation réfléchie saisie dans l'image Landsat TM du 7 mai 1988. Les spectres de réflectance de terrain ont été utilisés pour l'analyse

des images Landsat TM. Les résultats de la déconvolution spectrale se rapportent bien aux estimations obtenues dans le terrain. Les unités de recherche ont montré une tendance à une couverture d'herbes mortes au détriment du sable nu pendant les dernières années. Cette tendance correspond à la présence des champs agricoles abandonnés à cause d'une fertilité diminuée après une culture intensive.

Introduction

Population growth and man-induced climatic change makes life in the Sahelian countries even tougher. The increased pressure on land is a threat to the ecosystem of the sahel. Overgrazing and decreased soil fertility lead to erosion and poor harvests. To tackle these serious problems, it is necessary to find methods to map these degradation features. This can also help to understand the different processes.

Degradation of land often expresses itself in a change in the amount and distribution of earth-surface properties. For example, increased degradation in semi-arid areas leads to an increased area of crusted surfaces. Traditional image classification techniques do not give quantified measurements of soil surface characteristics.

Desertification is one of the major causes of degradation in the Sahelian countries. It expresses itself as an increase in erosion and a decrease in the vegetated area.

The processes of degradation are often active on a sub-pixel scale. The spatial variation of most landunits is very high, the range of the semivariogram of land qualities and reflectance in these areas is 7 to 10 meters. With pixels larger than 10 meters it is not possible to map terrain differences within the mapping units (EPEMA and BOM, 1994). Special image processing techniques are required to extract this detailed information from satellite images. In this research the possibilities of spectral unmixing with broad available Landsat TM data are examined.

The study area

The study area is located in the department Sanmatenga. The department was mapped as part of a co-operation of the *Antenne Sahélienne* of the University of Wageningen (The Netherlands), and the development organisation PEDI, financed by the Dutch government. Apart from the research presented in this paper, a soil map, vegetation map and land evaluation map are produced at a scale of 1:100,000. The mapping is carried out with the aid of multitemporal satellite images.

The area covers mainly the geologic time zones Birrimien and anti-Birrimien. The main rock of the Birrimien is schist and of the anti-Birrimien granite and granodiorite.

Due to past and present ferralitisation, there are hardened plinthite plateaus and layers throughout the area (ELKENBRACHT *et al.*, 1995). The ferralitisation in combination with ferrolyse, clay transport, erosion and leaching results in large differences in soil characteristics in the horizontal and vertical. Differences in texture and available nutrients lead to differences in fertility and vulnerability to erosion. The soils of the Birrimien are more fertile than those of the anti-Birrimien. The type and amount of clay minerals, organic matter and slope determine the erosivity of soil units.

Spectral characteristics of soil and vegetation

Each object on earth has its own spectral reflectance due to the chemical composition of the object. Objects can be discriminated by their spectral reflectance, caused by the reflectance of solar radiation. Light emitted by the sun interacts with the object and part of that light is reflected in the direction of the sensor. Various algorithms have been developed to differentiate between different objects. In the next part the different characteristics, which influence the reflectance of soils, green and dead vegetation, are briefly summarised.

Soils

The reflectance of soils depends on texture, structure, minerals, organic matter and water content. Some characteristics lead to an overall decrease in reflectance, others absorb radiation in a more specific wavelength. With hyper spectral (airborne and in the future spaceborne) radiometers it is possible to detect individual absorption features. Satellites, like Landsat TM, measure the reflectance in broad absorption bands, hiding these features. Absorption features, present in bare soil spectra, are mostly caused by iron oxides and OH-bearing minerals. Iron oxides cause a broad absorption dip around 900 nm, OH and CO_3-bearing minerals more narrow dips between 2,000 and 2,500 nm.

Healthy vegetation

Healthy vegetation absorbs a lot of radiance in the visible part of the spectrum for photosynthesis. The absorption is lowest in green (500 nm), therefore vegetation is green for the human observer. The reflectance in the near infrared is very high, due to the physiological structure of the leaves.

Dead vegetation

Dead vegetation lacks the high absorption in the visible, and the reflectance is highest around 1,600 nm (Landsat TM band 5). The spectral reflectance gently increases until 1,600 nm after which it decreases.

Data sources

Field data

The spectral reflectance of different surfaces is measured in the field with the mini-IRIS RT (GER2100) field spectrometer of the Geophysical Environmental Research corporation (GER, 1992). This instrument measures in 140 wavelength bands between 400 and 2,500 nm. It is a single field of view instrument, so a calibration plate is used to determine the incoming radiation. Depending on the research, there are two measurement types:

- 76 bands between 400 and 1,100 nm, 64 bands between 1,100 and 2,500 nm;
- 76 bands between 400 and 1,100 nm, 64 bands between 2,000 and 2,500 nm.

The advantage of grating 2 is the very high spectral resolution (8 nm) in the part of the spectrum where the discrimination of different minerals is possible.

The viewing angle is 6.5 degrees. A 120 cm instrument height results in a pixel size of 27 x 27 cm.

Image data

For this research it was possible to use different Landsat TM images. Available were images of the following dates: January 10, 1991; May 7 1988 and September 20, 1988. Since most interest went to bare soil surfaces, the January and May images, both of the dry season, were found most suitable. Bare soil differences are well expressed in those images.

Data processing and discussion

Resampling of field spectra

To use field spectra as endmember for unmixing of Landsat TM data, it is necessary to resample the spectra to TM wavelength bands. The overall form of the spectral curve is preserved but the specific absorption features, detectable with the field spectrometer, are not visible after resampling. In figure 1, typical spectral curves of objects present in the study area with the positions of the TM wavelength bands are shown.

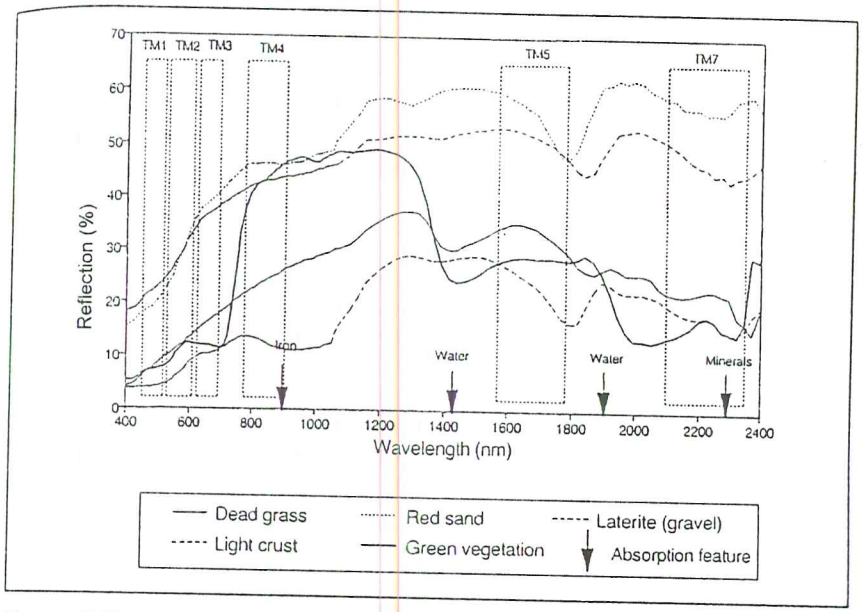

Figure 1. Different spectral curves of surfaces in the study area.

Geometric and spectral correction of image

Spectra collected in the field can only be used when correlation between the satellite data and the field data is high. To determine this correlation, the "empirical line method" is used. This, mathematically, relative simple spectral correction method proved to be very reliable (e.g. CONEL *et al.*, 1987 and FARRAND *et al.*, 1994). The regression parameters can be used to calculate field reflectance with the dimensionless Digital Number (DN) values of the satellite data.

Resampled field reflectance spectra of different surfaces are collected in the field and compared with the Landsat TM data. The location of the areas of interest is determined visually on hardcopies of the image and with the aid of a Global Position System. Areas with high and low reflectance are used to find the gain and offset for each of the Landsat TM bands. In figures 2 and 3, two examples of the correlation between mini-IRIS data and Landsat TM data of May 1988 are shown.

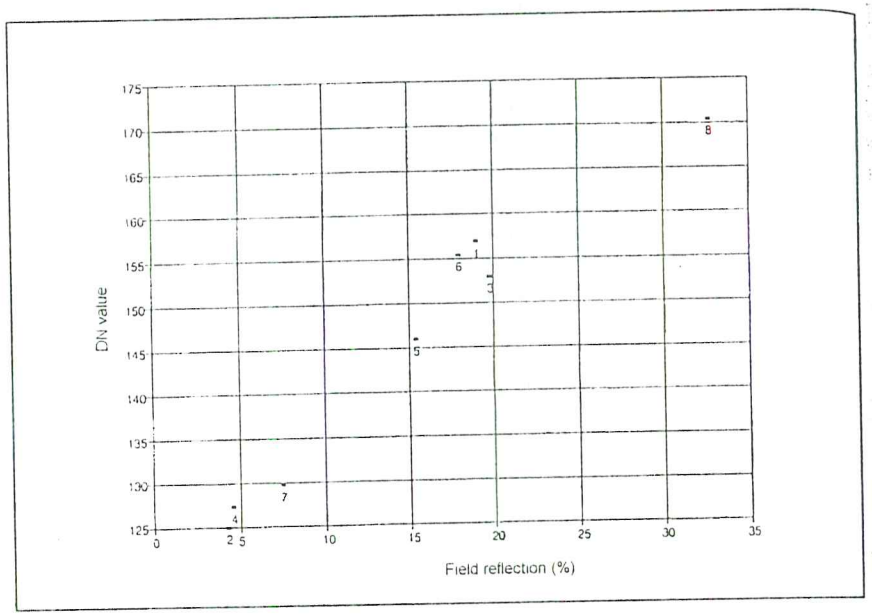

Figure 2. Correlation between Landsat band 1 of May 7, 1988 and field reflectance.

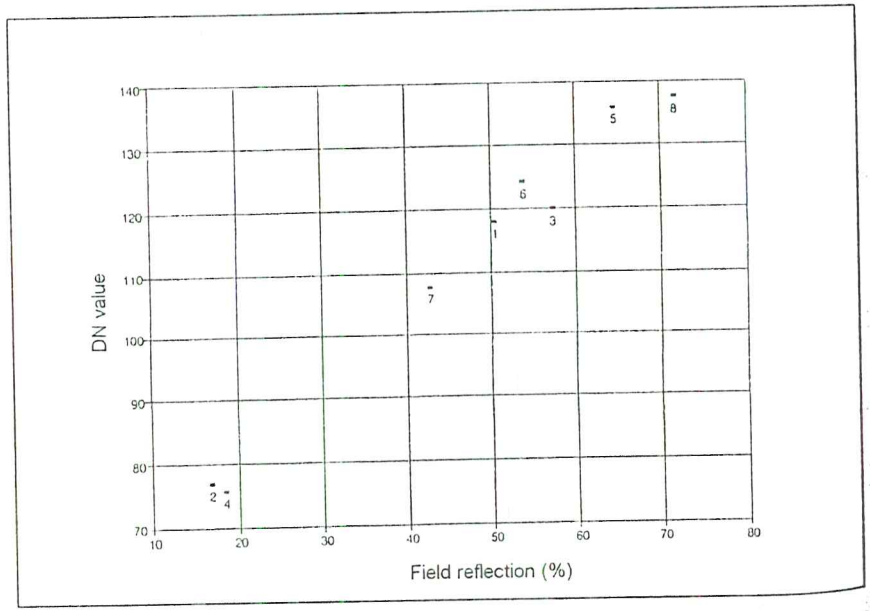

Figure 3. Correlation between Landsat band 7 of May 7, 1988 and field reflectance.

The regression parameters found with the empirical line method seemed very good. However, large differences were found between field reflectance spectra and image spectra outside the area where the training pixels were sampled. In spite of the fact that no albedo differences were visible on hardcopies of the May 1988 image, there were considerable differences in DN values of the same objects in different locations in the image. After careful examination of the raw TM data, differences of 5 - 25 DN were found. Surfaces with a low albedo, located in the North of the area, showed the largest differences. The DN differences were highest in band 5. In figures 4 and 5 respectively the DN values of laterite (gravel)- and crusts-pixels are shown for various locations. The locations of the villages range from Kaya in the South to Dablo in the North. The differences of light coloured, crusted surfaces are less than the differences of the laterite (gravel) surfaces. The differences are probably caused by the harmattan dust. This dust is blown from the Chad basin to the Sahel during the dry periods (McTRAINSH and WALKER, 1982). Because the dust is very light coloured, the influence on the reflection is higher above dark surfaces.

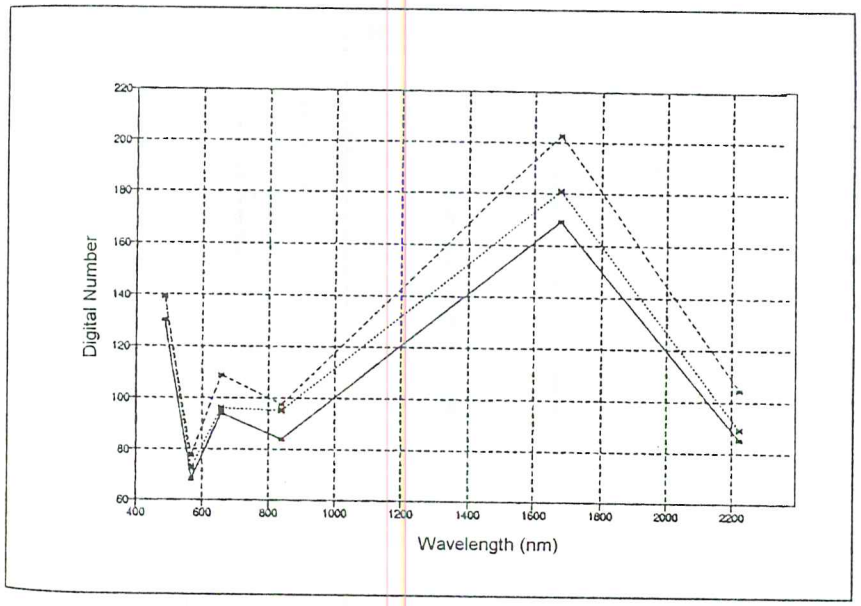

Figure 4. Differences in reflectance of (laterite) gravel due to the influence of harmattan dust in the air.

For the unmixing process Landsat TM bands 1, 2, 3, 4, 5 and 7 of January 10 1991 are used. In this image no influences of the harmattan dust were found. The pixel DN values were processed to field reflection using regression parameters found with the empirical line method.

Selection and comparison of endmembers

During the fieldwork, surfaces present in the different landunits are detected and the reflectance of these surfaces is measured with a field reflectance meter.

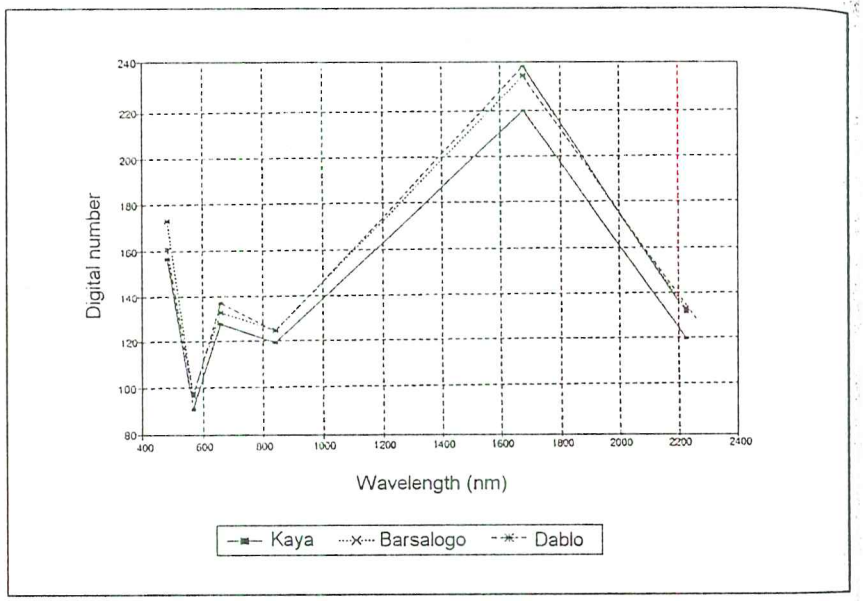

Figure 5. Differences in reflectance of light coloured crusts due to the influence of harmattan dust in the air.

The selection of endmembers is based on the following considerations:

- Due to the co-operation with PEDI, the most important areas of research are those where agriculture can be initialised or is present. For this reason, unsuitable units, e.g. hardened plinthite plateaus, have been excluded as endmembers.

- Shade endmembers are often used to reduce the effects of differences in illumination through differences in slope steepness and direction (GILLESPIE *et al.*, 1990). As the relief in the study area is limited, the exclusion of this endmember is permissible.

- Endmembers often absent in pixels are not included, while this leads to an overestimation of this endmember.

- As mentioned before, the number of endmembers is limited by the number of spectral bands.

To determine the similarity of the endmembers, two methods are used. The euclidean distance is sensitive for similarity in overall reflectance of endmembers. The spectral angle determines the similarity of the form of spectra (KRUSE *et al.*, 1993). Figures 6 and 7 show

respectively the euclidean distance and the spectral angle between the different endmembers. The values can forecast which endmembers are likely to be confused with each other.

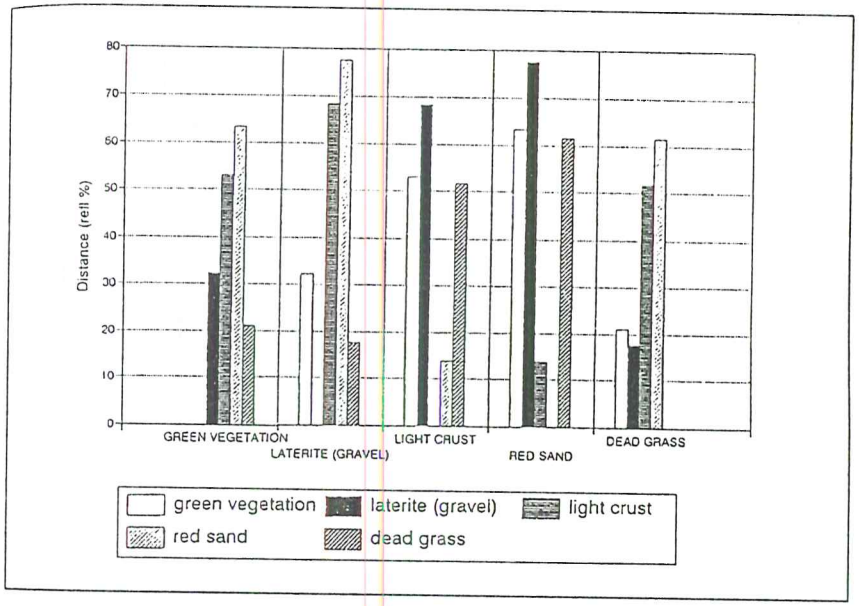

Figure 6. Euclidean distance between endmembers.

Albedo differences cause high differences in euclidean distance between light and dark endmembers. In general, green vegetation and laterite resemble dead grass and light crust resembles red sand. A low spectral angle between two endmembers is likely to cause problems with the calculation of the fractions of the two endmembers.

Spectral unmixing

Most objects on earth have a dimension smaller than the spatial resolution of present satellites. Pixels are composed of different objects each with its own spectral characteristics. Reflectance spectra can be modelled as a mixture of a few, so called endmember spectra (ADAMS *et al.*, 1989). Endmember spectra are the individual reflectance spectra of the different objects present in the pixel. The spectral variation in an image is caused by a limited number of surface materials like soil types, vegetation types and shade. Spectral mixture analysis is, up to now, mostly used with airborne hyper-spectral airborne data like AVIRIS and GERIS. Less emphasis is put on the use of this relative new technique with satellite data. SPOT data has the disadvantage of having only three spectral bands, which will (due to constraints in the calculations of

unmixing) limit the amount of used endmembers to two. With this limited amount of endmembers it is not possible to describe the variability of the image. On the other hand, Landsat TM has, for most occasions, enough spectral bands to execute spectral unmixing.

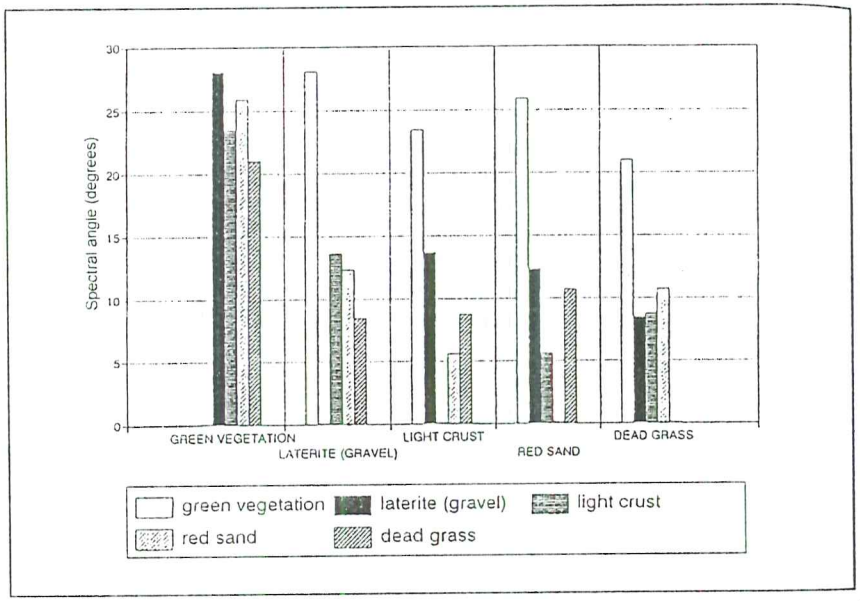

Figure 7. Spectral angle between endmembers.

As an approximation, the spectral mixing can be modelled as a linear combination of the pure endmember spectra, as follows:

$$R_i = \sum_{j=1}^{m} (F_j \cdot RE_{ij}) + e_i \wedge \sum_{j=1}^{m} F_j = 1 \wedge 0 \le F_j \le 1 \qquad (1)$$

where:

R_i : reflectance of the mixed spectrum in band i;
RE_{ij} : reflectance in band i of endmember j;
F_j : fraction of endmember j;
m : number of endmembers;
e_i : residual error in band i;

The above expression has a solution when the number of endmembers does not exceed the number of spectral bands minus one. Linear mixing occurs when the components are large or opaque enough to allow photons to interact with only one component (SINGER and MCCORD, 1979). The mathematical solution of the above

expression can be validated by examining the difference between the calculated and measured reflectance by the root-mean-squared (RMS) error.

$$RMS = \sqrt{\sum_{i=1}^{n} (R_i - R'_i)^2} \qquad (2)$$

where:

R_i : modelled or predicted reflectance of the pixel in band i;
R'_i : measured reflectance of the pixel in band i;
n : number of spectral bands.

The RMS error gives information about the amount of spectral variability explained by the selected endmembers. When the reflectance of a pixel can not be modelled by linear mixing with the selected endmembers, this will lead to a high RMS error.

As an example, the unmixing results of an area near Dablo in the North of Sanmatenga are examined. Resampled spectral curves, shown in figure 1, are used as endmembers in the unmixing. The processing of the image is done with the program Spectral Image Processing System (CSES, 1993) on a DEC Alpha 166 MHz. The processing time was 420 pixels per second with a 100% CPU time.

In plate 8, five images with each the distribution of a endmembers are shown. The minimum and maximum values used for stretching are given. The lighter the grey tone, the higher the coverage with the corresponding endmember. Some surfaces like green vegetation, light crusts and dead grass show high differences in coverage throughout the area. Laterite (gravel) and red sand are found in the whole area. This has to do with the processes that cause the forming of these surfaces. In the dead grass image, a striping is seen. Dead grass has a typical high reflection in band 5. The original striping is present in band 5. A high band 5 DN, caused by the low signal to noise ratio of this band, gives the spectral curve of a pixel the form of dead grass. The contribution of dead grass in that pixel is then overestimated. A too low band 5 DN, results in a spectrum that differs from dead grass. The dead grass coverage is then underestimated.

The crusted surface is highest at the south-west side of the laterite plateau. This side of the plateau is characterised by a crest. The geologic layer underneath the hardened plinthite layer is rich in kaolinite. This kaolinite, in combination with the slope, results in erosion and crusting of the soil.

During the fieldwork the coverage of endmembers is estimated for different sites. The estimates are compared with the unmixing results. In figures 8 to 11 these comparisons are visualised for four sites.

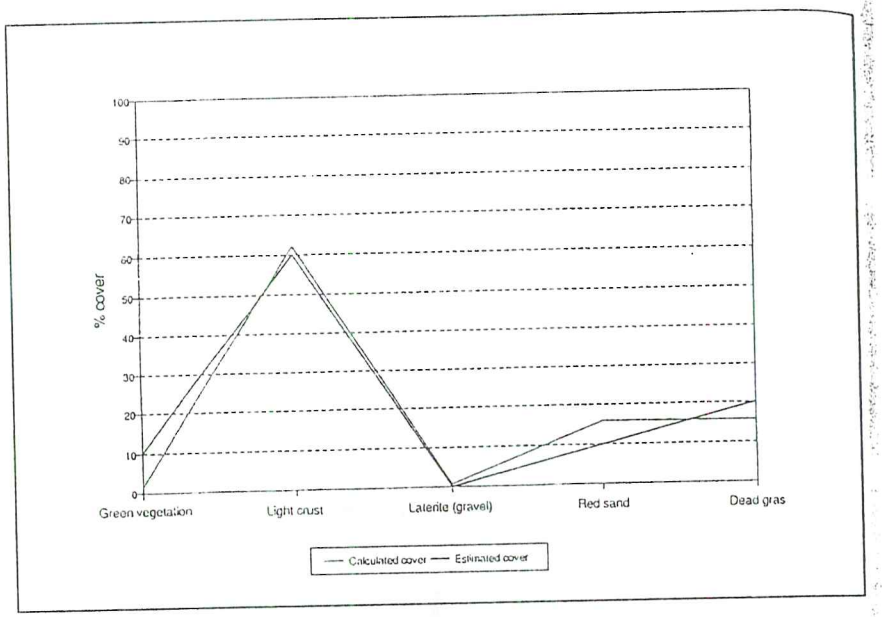

Figure 8. Ground cover near Barsalogo.

The calculated coverage with red sand is in all test sites higher than estimated in the field. On the other hand is the dead grass coverage underestimated. The image used in this research is from February 1991, the fieldwork was in October 1994. The time difference is therefore about four years. During the fieldwork, several sites are found with deserted agricultural fields. The sand of these fields seems to be replaced by dead grass. The high grass coverage is also caused by the relative wet rainy season of 1994. Other possible causes of the differences found between field estimations and unmixing calculations are mentioned below:

- Errors in the determination of the regression parameters used for spectral correction;
- The spectra of the endmembers are based on a good average spectra measured in the field. These average spectra might not be used for description of surfaces which have a slightly other reflection. The deviant reflection can cause wrong unmixing results.
- The combination of endmembers is not such that it is possible to describe the different units.

After the unmixing process, the five endmember images were unsupervised classified. The clusters represent relative homogeneous units. Figure 12 gives the average composition of 6 from in total 10 clusters of the Dablo area. The statistics of these clusters give information about the average distribution of endmembers. With this method, the classified image contains direct information about the constitution of the units. This information can be very useful for applications where specific, quantitative information about units is necessary. Possible applications are: decisions about the position of mapping boundaries, more specific remote sensing data input for erosion and other models.

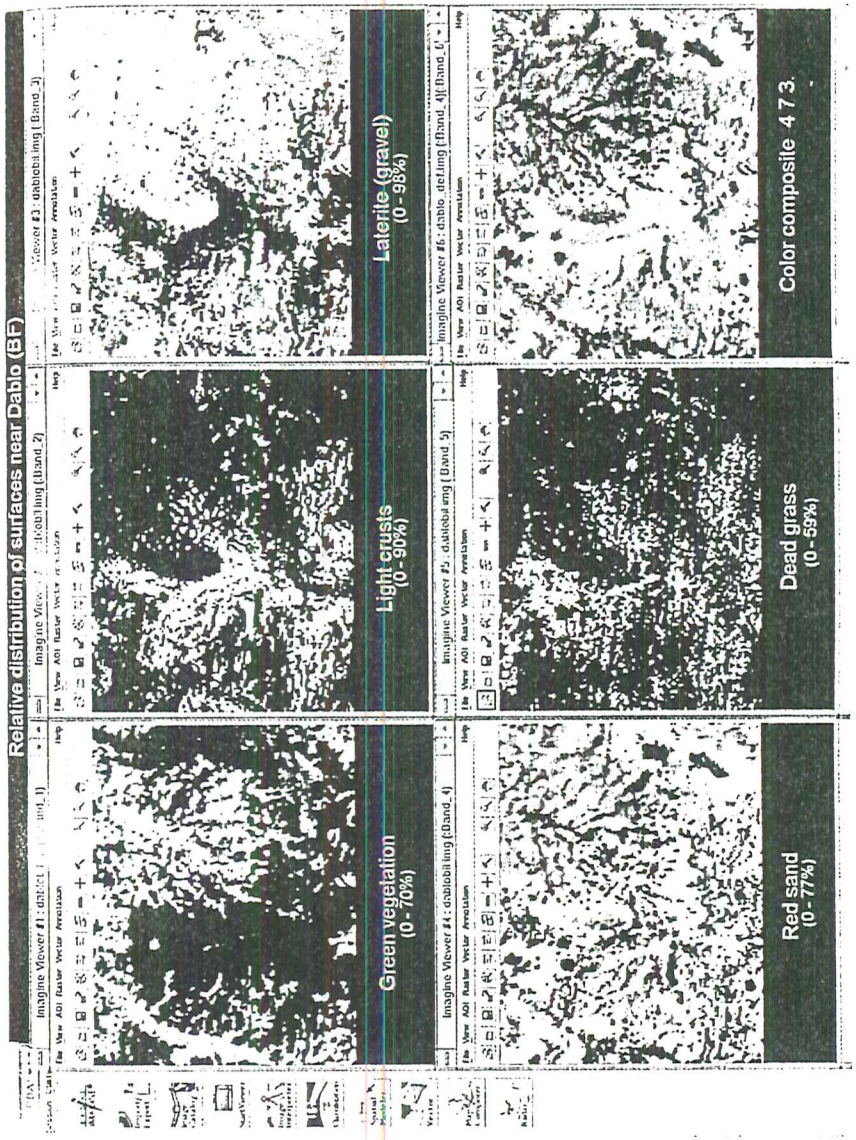

Plate 8. Spatial distribution of endmembers in the test site near Dablo in Burkina Faso (p. 279).

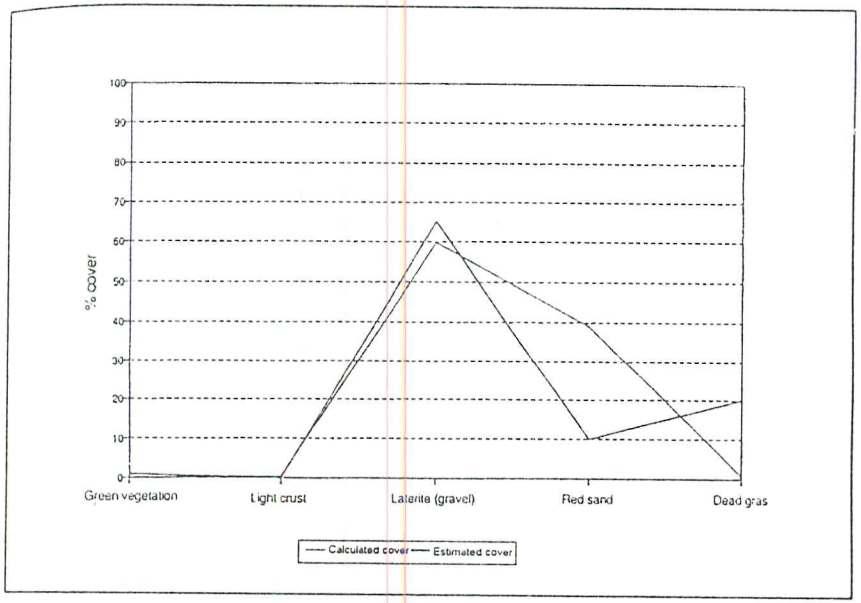

Figure 9. Ground cover Dablo site 1.

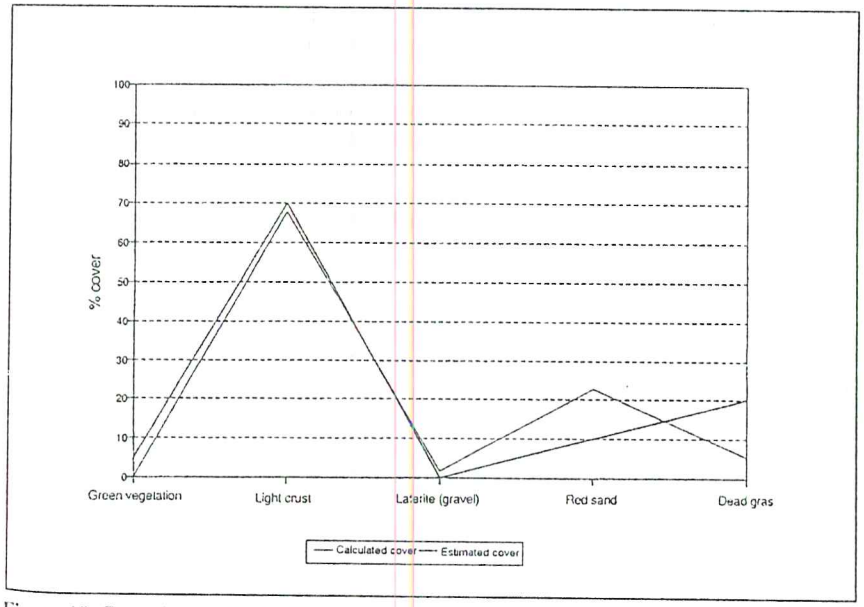

Figure 10. Ground cover Dablo site 2.

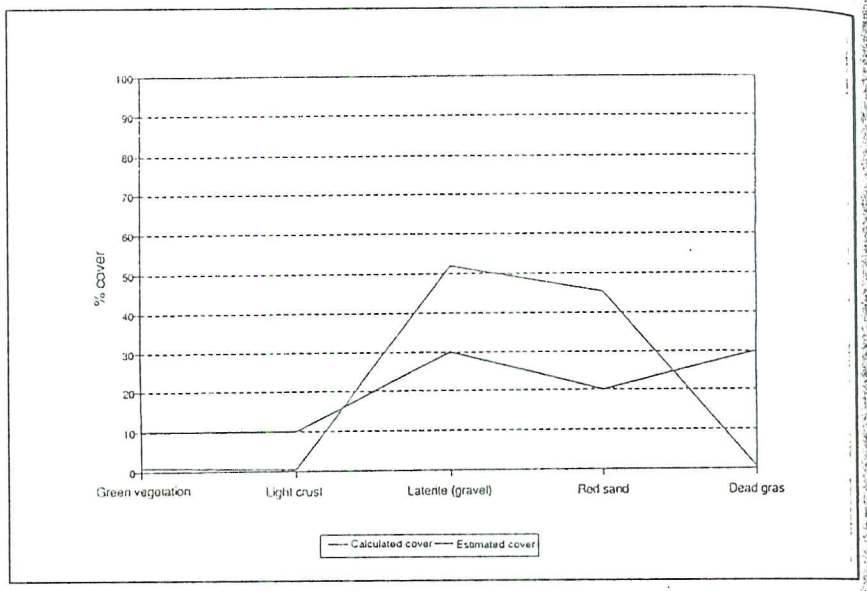

Figure 11. Ground cover Dablo site 5.

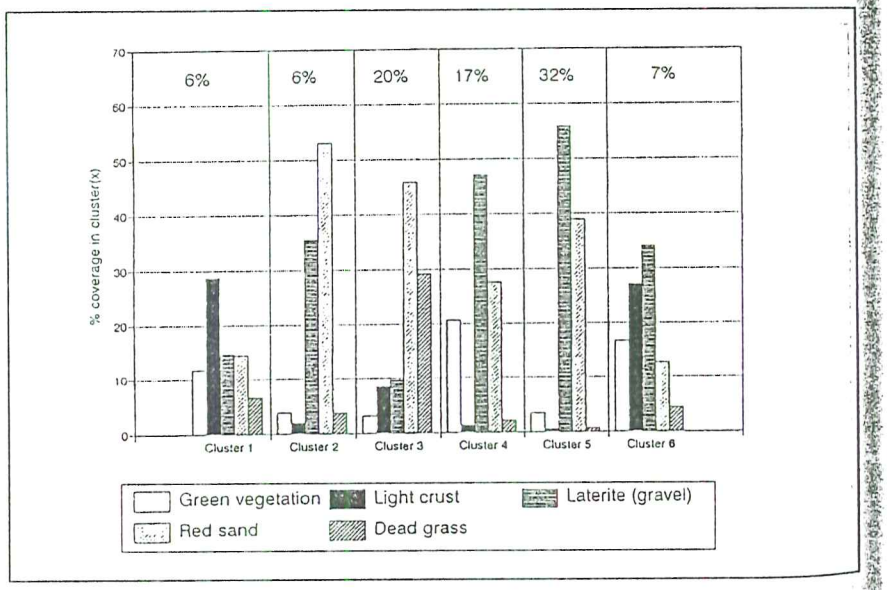

Figure 12. Average composition of 6 clusters. Numbers above bars give the total area in percentage, covered by the clusters.

Cluster 5 has, with 32% of the area, the highest coverage. This cluster represents the laterite plateaus and areas with a high coverage of laterite gravel. Clusters 3 and 4 also have a relative high coverage with laterite gravel. Cluster 4 is located in the so called *bas-fond*, the valley with relative dense (tree) vegetation. The 21% vegetation might be underestimated because of the shade of the trees. This shade will, due to the lowering in overall reflectance of the pixel, contribute to the percentage laterite.

Conclusions and recommendations

In the Sahel, the presence of harmattan dust in the air can influence the reflection of the surface, even if there is no influence visible at first sight. The data should be carefully examined before any data processing is started.

The use of field reflectance spectra is possible, when good regression parameters are found, e.g. with the empirical line method, to correct the digital numbers of the satellite image.

The first unmixing results show a quite good correspondence between field estimates and calculations. Differences can be caused by:

- Changes in landcover during the time of recording of the image and the time of fieldwork;
- The regression parameters found with e.g. the empirical line method can be wrong;
- The endmembers used are not representative for surfaces that have a slightly different reflection.

Clustering of the images with the distribution of endmembers, results in useful additive information about classification units.

To unmix Landsat TM images of complex landscapes, a first subdivision in mayor units is necessary. The units can then be unmixed each with their own selection of endmembers.

In further research, a sensitivity analysis is necessary to determine the influence on the final results of each step in the unmixing procedure.

References

ADAMS J.B., SMITH M.O., GILLESPIE A.R. (1989). "Simple models for complex natural surfaces: a strategy for the hyperspectral era of remote sensing", in: *Proc. IEEE Int. Geosci. and Remote Sensing Symp. '89 I*, IEEE, New York, pp. 16-21.

CONEL J.E., GREEN R.O., VANE G., BRUEGGE C.J., ALLEY R.E. (1987). "AIS-2 radiometry and a comparison of methods for the recovery of ground reflectance", in: *Proc. 3rd Airborne Imaging Spectrometer Data Analysis Workshop* (G. Vane, Ed.), JPL Publication 90-54, Jet Propulsion Laboratory, Pasadena, CA, pp. 18-47.

CSES (1993). *SIPS User's guide*, Spectral Image Processing System Version 1.2, Center for the study of Earth from space (CSES) and Cooperative Institute for Research in Environmental Sciences (CIRES), University of Colorado, Boulder.

ELKENBRACHT E. HOLTETEN A., OTTER L., SLAA T. (1995). "Remote sensing and soil science in the Kaya area (Burkina Faso)". *Antenne Sahélienne report 34*, Wageningen Agricultural University, The Netherlands.

EPEMA G.F., BOM B.C.J. (1994). "Spatial and temporal variability of field reflectance as a basis for deriving soil surface characteristics from multiscale remote sensing data in Niger", *ITC Journal* 1994-1, pp. 23-28.

FARRAND W.H., SINGER R.B., MERENYI E. (1994). "Retrieval of apparent surface reflectance from AVIRIS data: A comparison of empirical line, radiative transfer, and spectral mixture methods", *Remote Sens. Environ.* 47:311-321

Geophysical & Environmental Research corp. (1993). Operation manual GER'S mini-IRIS RT spectroradiometer, 23 p.

GILLESPIE A.R., SMITH M.O., ADAMS J.B., WILLIS S.C., FISCHER A.F., SABOL D.E. (1990). "Interpretation of residual images: Spectral mixture analysis of AVIRIS images", Owens Valley, California, in: *Proc. 2nd Airborne Visible/Infrared Imaging Spectrometer (AVIRIS) Workshop* (R.O. Green, Ed.), JPL Publication 90-54, Jet Propulsion Laboratory, Pasadena, CA, pp. 243-270.

KRUSE F.A., LEFKOFF A.B., BOARDMAN J.W., HEIDEBRECHT K.B., SHAPIRO A.T., BARLOON P.J., GOETZ A.F.H. (1993). "The Spectral Image Processing system (SIPS) - Interactive visualisation and analysis of imaging spectrometer data", *Remote Sens. Environ.* 44:145-163

MCTRAINSH G.H., WALKER P.H. (1982). Nature and distribution of harmattan dust, *Z. Geomorph.* N.F. 26 (4):417-435, Berlin.

SINGER R.B., MCCORD T.B. (1979). "Mars: large scale mixing of bright and dark surface materials and implications for analysis of spectral reflectance", in: *Proc. 10th Lunar Planetary Sci. Conf., J. Geophys. Res. Suppl.*: 1835-1848.

Getting Insight into Soils and Land with M.A.S.I.S. : a Proposed Methodology in a Remote Sensing - GIS Environment: a Case Study of the Manga Area, Burkina Faso

Tomas LAGUNA-GOMEZ

Dpto. Ciencias del Suelo y Medio Ambiente, Universidad de Lleida, Spain.
Department of Soil Science and Geology, Agricultural University of Wageningen, The Netherlands.

Abstract

The present work is an example of how to take much profit out of a very powerful GIS, using data from different sources without any previous knowledge about the particular way of working with any software package. It may serve as a method supporting the work of scientists and engineers active in studying the environment.

Résumé

Le présent travail est un exemple qui montre comment tirer profit d'un puissant SIG en employant différentes sources de données -sans aucune connaissance préalable de l'utilisation d'un logiciel de ce type. Il peut servir de méthode pour aider le travail des scientifiques et ingénieurs qui étudient l'environnement.

Introduction

Every soil-scientist appreciates the role of airphoto-interpretation for soil mapping and land evaluation. Nevertheless, especially when large new areas need to be surveyed and little information is available, satellite imagery can play an important role when planning the

field work (BUITEN and CLEVERS, 1993) in order to save time and money, but also for improving the accuracy of the final results. The use of Geographical Information Systems (GIS) for the storage, management, analysis and presentation of geographic and thematic data is a powerful tool in the process of "getting insight into soils" and their position in the landscape. A soil scientist should know about the possibilities of GIS, and take the maximum profit out of them, but cannot be expected to spent much time in learning a very complex commercial software package.

Objectives

The present work is the result of a research with two main objectives:

- The development of an easy way to handle much information taking profit out of a very powerful GIS using data from different sources without any previous knowledge about it. It may serve as a method supporting the work of scientists and engineers active in studying the environment;
- Evaluate the possibilities of GIS for erosion modelling and assessment. Surface analysis and hydrologic modelling using a DEM (Digital Elevation Model) are studied in order to be combined with remote sending data.

Methods

Airphoto-interpretation was made according to the traditional practices (MULDERS, 1987); thematic field work was stored in a database installed on a portable computer, and later on included in the GIS geographic database; remotely sensed data was processed and classified with ERDAS (ERDAS, 1991). In ARC/INFO v.6.1.1, a Digital Elevation Model (DEM) was created and analysed, not only for surface but also for hydrologic modelling (MARTINEZ, 1994). The coverages were digitized in ARC/INFO, as well as the program M.A.S.I.S. (Manga Area Soil Information System) was written. It was also the environment where all the data were combined and read.

Information generated by airphoto-interpretation, fieldwork, processing of satellite imagery and derived from a DEM are combined in a GIS environment. The result is a program that enables, with the use of only one key on a computer mouse, the display of remotely sensed data, the overlay of digitized coverages (maps, drainage network, roads and villages,...) both on the processed satellite data and on the DEM and most important, the making of queries by attribute or by location, and generating statistics about the extracted information.

Main results

- Remote Sensing used in combination with Geographic Information Systems is a useful data collection system to provide accurate information on the variables controlling the land degradation processes. Erosion assessment can be improved using a Digital Elevation Model.

- Information generated with remote sensing, GIS and other well proved techniques can be combined and made easily accessible. M.A.S.I.S. is an easy program written with the Arc Macro Language of ARC/INFO. It is a simple but effective soil information system with the following main options:

- About the study area : Topographic information on Burkina Faso, Zoundweogo (province) and Manga (study area).
- Display of ERDAS formatted imagery (ERDAS .LAN, .GIS) on screen;
- Display ARC/INFO coverages on screen;
- Query the information system by attribute : The program allows to use a backenvironment to guide the queries. With specific overlays on physiography and vegetation, the terrain data base with field characteristics can be consulted, formulated by logical expressions.
- Query the information system by location : Select backenvironment and overlay and make queries by location (points or area).
- Information about M.A.S.I.S.;
- End the session;
- Fly over the study area : Specific views derived from the DEM can be selected for inspection.
- Study some topographic profiles : Selected cross sections derived from DEM processing.

Some examples are given below to illustrate the program.

A DEM was developed from existing cartographic data. It was converted into a raster in order to calculate slopes and aspects (slope and water flow direction); then the water flow accumulation and as a result the drainage pattern.

Fig. 1 shows the drainage pattern derived from aerial photo-interpretation as well as estimated from the Digital Elevation Model by ARC/INFO software. The latter has high potential for analyzing the preferent directions in the system to get knowledge about the relationship of drainage pattern with geology.

ARC/INFO has a lot of possibilities for producing informative maps, such as a flow accumulation map (characterizing runoff) and sunshaded relief (Fig. 2). This view of the area is manipulated to exaggerate the height differences and serves geomorphic interpretation.

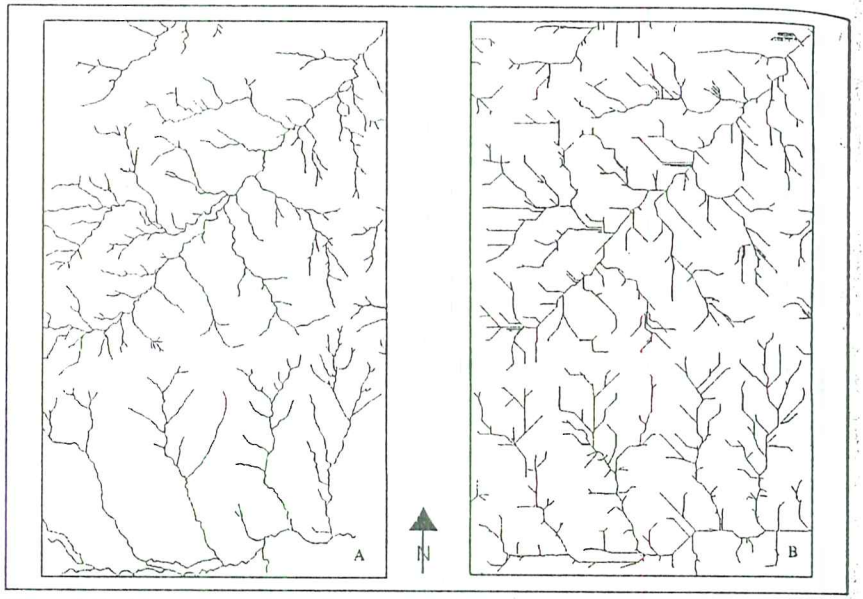

Figure 1. Drainage network of the Manga area (Kaibo) derived from aerial photo-interpretation (A) and from the DEM in ARC/INFO (B). *Le réseau de drainage dérivé du MNT comparé avec la photo-interprétation aérienne.*

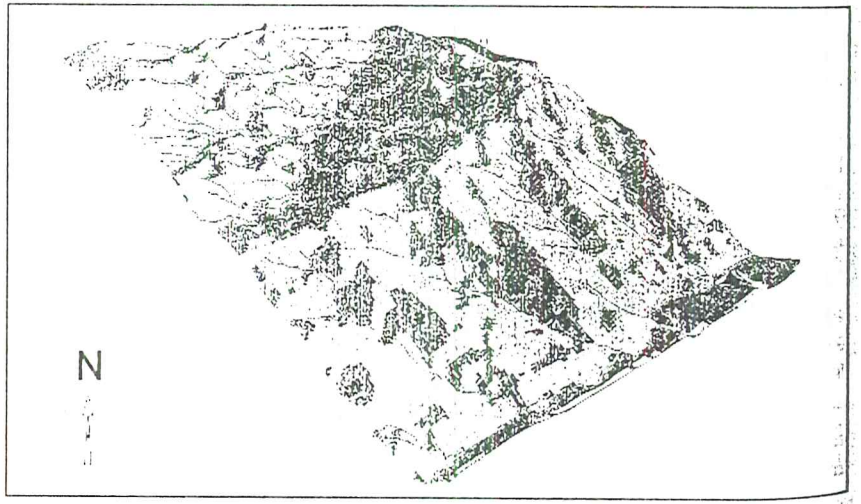

Figure 2. The Manga (Kaibo) area seen from the south-west, visualized by draping a sun-shaded relief grid and drainage network from aerial photo-interpretation. *La région d'étude vue du sud-ouest, par la superposition du relief ombré et du réseau de drainage.*

Conclusions

Different coverages are made easy accessible in the program. Queries may be done to study land cover and soils, e.g. the % of coverage of trees, shrubs, herbs and soil characteristics are given by location since these data are made accessible.

The program proved to be very useful in the preparation of preliminary land cover and physiographic maps, the testing of validity of the available data on soils and land cover and in the preparation of a second phase of field work in planning sites for field observations.

References

BUITEN H.J., CLEVERS J.G.P.W. (Ed.), (1993). *Land observation by remote sensing. Theory and applications*. Gordon and Breach Science Publ., Amsterdam, The Netherlands.

ERDAS Inc. (1991). *ERDAS Field Guide and user's manual, v. 7.5*. Atlanta, USA.

MARTINEZ J.A. (1994). *Hydrographic information abstraction for erosion modelling at regional level*. MSc Thesis in GISRA Course. ITC Enschede and Wageningen Agric. Univ., The Netherlands.

MULDERS M.A. (1987). "Remote Sensing in Soil Science", Developments in Soil Science 15, Elsevier Science Publishers B.V., Amsterdam, The Netherlands.

Excursion To The Kaya Region, Burkina Faso

P.N. ZOMBRÉ, F. PALLO, M.A. MULDERS, L. THIOMBIANO, L. STROOSNIJDER, W.B. HOOG-MOED, M. TROMP, B.R. KABORÉ, J.H.V. VAN BAREN

1. Burkina Faso

1.1. FAO-UNESCO Soil Map of the World

The production of the Soil Map of the World at scale 1:5,000,000 began in 1961 on recommendation of the International Society of Soil Science (ISSS) at the Congress in Madison (USA, 1960).

The main objective was to make an overall world inventory of the soil resources in order to face the problems of land degradation, inequality of production potential and demographic charge capacity, which became international issues at that time.

1.2. Pedological units Burkina Faso

The different pedological units, represented on the Africa sheet of the Soil Map of the World (FAO-UNESCO, 1976), are given in table 1.

Table 1. Pedological units of the Soil Map of the World, Burkina Faso.

Units	Area in km^2	Subunits
Luvisols	126,810	Plinthic, Ferric, Gleyic
Regosols	74,780	Eutric, Dystric
Cambisols	16,000	Vertic, Eutric
Vertisols	13,850	Chromic, Pellic
Planosols	12,660	Solodic
Arenosol	12,570	Luvic, Cambic
Lithosols	8,390	
Nitosols	3,090	Dystric
Acrisols	1,110	Plinthic

1.3. Global assessment of soil degradation with reference to Burkina Faso

The United Nations Environment Program (UNEP) signed a contract with the International Soil Reference and Information Centre (ISRIC, Wageningen, The Netherlands) for the preparation of a global assessment of the state of human-induced soil degradation at a scale of about 1:10,000,000.

Regional maps (Fig. 1) were collected and correlated to construct soil degradation map at exploratory scale. The Global Assessment of Soil Degradation (GLASOD) was published with an explanatory text in 1990 and 1991. This work was also used for the World Atlas of Desertification, published for UNEP in 1992.

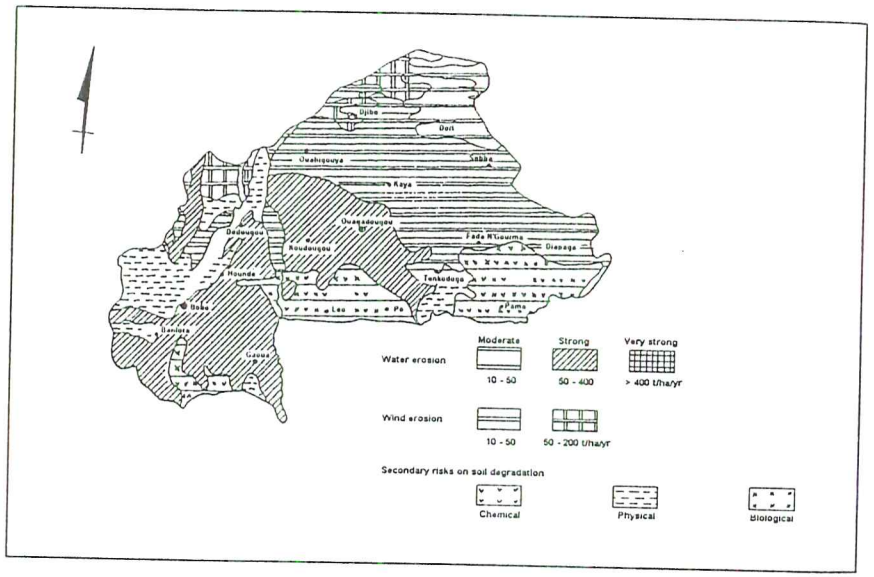

Figure 1. Risk of soil degradation in Burkina Faso according to FAO-UNEP-UNESCO (1980).

1.4. Overview on physical and human environment

1.4.1. Situation and climate

Burkina Faso is a country in the middle of West Africa. The total area is 274,000 km². The climate is Sahelo-Sudanese with an average annual rainfall of 400 mm in the north and 1200 mm in the south near to Ivory Coast. The isohyets are given in figure 2.

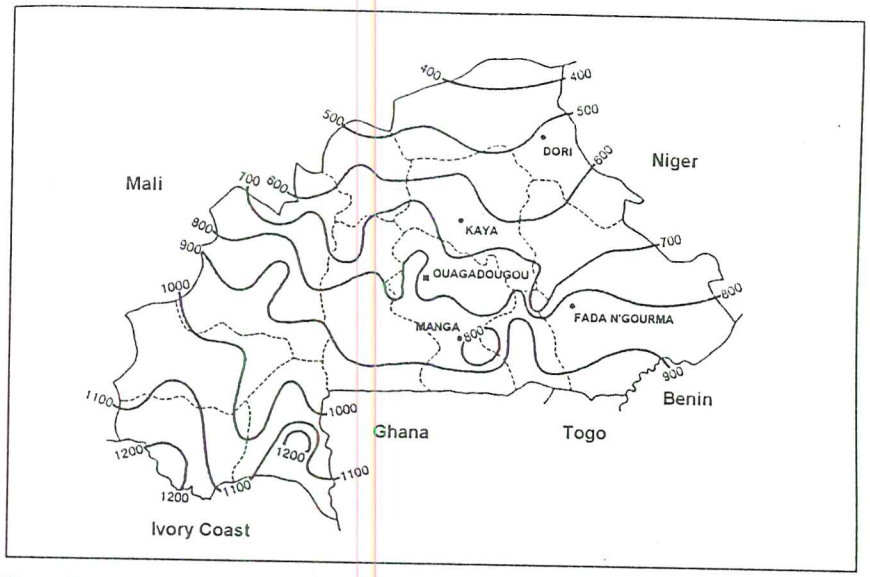

Figure 2. Isohyets of Burkina Faso.

1.4.2. Topography, physiography and vegetation

The average height does not exceed 400 m with half of the country between 250 and 350 m. The soils are correlated with their geological origin:

- Soils of the African shield, usually gravelly and kaolinitic with low fertility, or montmorillonitic with high fertility but poor physical properties;
- Soils of the sedimentary basins, sands and sandy loams with low fertility or heavy textured with moderate fertility.

Burkina Faso is divided into two phytogeographical domains: the Sahelian and the Sudanese zones:

- The Sahelian zone is located north of the 14th latitude with an annual rainfall of less than 600 mm and is composed of steppes with discontinuous canopy of bush and annual *Poaceae*.
- The Sudanese zone is found south of the 14th latitude. In the centre of the country with 600-750 mm rainfall, a moderate coverage by trees, shrubs and perennial *Poaceae* are mainly found in the lowlands. The natural vegetation in the southern part of the country with rainfall more than 750 mm shows a relatively dense canopy of trees and shrubs, while forest is present in the lowlands.

1.4.3. Human environment

In 1988, the population was estimated at 8,556,000 inhabitants with an average density of 29 inhabitants per square kilometer and varying widely over the country. There is a large number of ethnic groups (about sixty) of which the main groups are according the 1985 population census: Mossi (48%), Fulbe or Peuhl (10%) and other groups, each less than 10%: Lobi, Samo, Bobo, Sénoufo, Gourounsi, Gourmatché and Bissa. These ethnic groups are characterized by differences in cultural background, land use and land ownership.

The population increase is very high with an increase of 41% from 1975 to 1985 and current increasing rate of 2.8% per year. Therefore, the population is extremely young: 54% had an age of less than 19 years in 1985. Urban evolution is also important: the urban population was about 6.4% of the total population in 1975, but in 1985 this proportion already was 12.7%.

2. Physical and human environment of the province Sanmatenga

2.1. Administrative situation

The Sanmatenga province belongs to the northern-central region between 12°40' and 14°N latitude. The city of Kaya is located at 100 km north-north-east of Ouagadougou and is the county town of the province. The province has an area of 9,419 km² or about 3.4% of the national territory. It is composed of 11 departments.

2.2 Climate

The climate is Sahelo-Sudanese with an annual rainfall of 500 mm in the north and 600 mm in the south. The dry season is from the middle of October up to the end of May, while the rainy season is from June to the middle of October.

The average temperature is between 27°C and 28°C with a minimum of 10.5°C and a maximum of 43°C. The temperature shows seasonal variations. There are two cold seasons (namely December to February and August) and two warm seasons, before and immediately after the rainy season.

From February to April, there is effect of a dry warm wind, the harmattan, issued from a Saharian anticyclone blowing from north to south.

2.3. Geology and soils

Two geological formations of the Precambrian are dominant. The Antebirrimian granitic formations are found in a more or less undulating landscape. They cover the

northern part of the province, extending to the south-east. The outcrops are composed of migmatites and calco-alcaline granites.

The Birrimian formations characterize the hilly subregions with schist and meta-volcano sedimentary formations.

The spatial split up of the pedological units largely follows the limits of the geological formations. The soils found range from well to poorly developed and can be hardened. Iron crusts are outcropping or covered by young soil material.

On the interfluvial tops of Birrimian hills, lithosols and poorly developed brown soils (Cambisols) are present.

2.4. Vegetation

The vegetation is globally characterized by savanna formations, often degraded.

In the south, *Butyrospermum paradoxum* trees are dominant besides low formations with *Combretum micranthum* and a relatively dense herbaceous cover under natural conditions.

In the north of the province, the savanna shows a Sahelian tendency with small shrubs, composed of *Combretaceae* and several thorny species. The herbaceous stratum contains mostly *Poaceae* in a discontinuous canopy, exposing bare soils with crusts, which hinder water infiltration.

The general distribution along toposequences is as follows: bushes occur at the tops and slopes of ironcapped mounts, crops and trees are found on faint slopes while tree lines are located along depressions.

A degraded vegetation condition results from combined effects of climate, rigorous cutting of trees, over-exploitation and agricultural and livestock pressure.

2.5 Social and economic environment

According to the results of the 1985 census, the population of Sanmatenga was 367,633 inhabitants with an average density of 39 inh/km² in the north against 56 inh/km² in the south of the province. The Kaya department had 67,104 inhabitants with a density of 69 inh/km². The province contained 357 villages, subdivided into 1,861 quarters, while 7% of the population lives in the county city.

Agriculture is the main activity for 80% of the population. Crop growing in order of decreasing importance is the following: millet, sorghum, cowpea, groundnuts and maize. Furthermore, garden production is significant.

The availability of agricultural land is low. The National Soils Bureau (BUNASOLS, 1990) estimated this to be 0.76 ha/farmer in this region.

Livestock holding is the second major activity. It is characterized by a "not-fixed grazing system." Arranged according to their decreasing importance, it concerns: goats, sheep and cows.

Important ligneous formations are observed in the protected forests of the province, namely: Dem, Nakambé and Yabo with a total area of 3,450 ha.

3. Kaya region

The Kaya region is located in the province of Sanmatenga; Silmiougou is a village in the centre of the excursion area at 4 km north of this town (for location, see Fig. 11).

3.1 Land use Silmiougou region

Diachronic analysis was done from two situations in the Silmiougou region:

- 1955 situation with aerial photographs of the AOF (French Occidental Africa) mission at 1:50,000 scale;
- 1994 situation with aerial photographs of IGB (Geographic Institute of Burkina Faso) mission at 1:10,000 scale.

Aerial photographic analysis of these photographs shows the widely spread environmental degradation.

In 1955, the area showed already a great rate of agricultural soil occupation (about 45%). Agricultural practices were concentrated in valleys and on faint slopes.

The area used for agriculture had strongly increased between 1955 and 1994: from 45% to 65%.

The lowlands, which are the moist and fertile zones, have been cleared and for more than 90% used for cropping. Hill slopes and tops were increasingly used for cropping, causing crusting, runoff and soil degradation. The 1994 condition showed extended areas with crusting and several barren zones, which were only used for extensive grazing.

The natural savanna vegetation had changed from 1955 to 1994: ligneous tree formations and small shrub savanna areas were reduced from about 50% to less than 10% of the total area.

3.2 Physical and chemical measurements on the degraded watershed of Silmiougou under sylvopastoral land use

3.2.1 General data

The study area consists of a 12.5 ha small (sub-)watershed directly north of Silmiougou. The average annual rainfall is about 650 mm. This watershed is heavily degraded, with a sparse vegetation of some shrubs, trees and grass.

In the Semi Arid Tropics very intensive rain showers occur (Fig. 3); about 15% of which has an intensity > 100 mm/hour (Fig. 4). The erosive power of showers increases

exponentially with the size of the showers (Fig. 5). For a shower of 40 mm the erosivity index EI30 is about 1,000 [J.mm/m².h] for each millimeter of rain and this value doubles till 2,000 [J.mm/m².h] for each millimeter of rain for a shower of 80 mm.

The landscape in Silmiougou is dominated by a very gentle long slope called *glacis*. The surface configuration of the watershed was determined, using various methods:

1. A topographic survey with a levelling instrument.
2. Constructing a digital height model using various types of software: SPATANAL (semi-variogrammes), MAPIT (geostatistical interpolation), SURFER (contours).
3. Import in a Geographical Information System (IDRISI 4.0).
4. Digitizing of surface phenomena (based on field observations) like crusts, gullies, annual and perennial vegetation using TOSCA.
5. Analysis of raw data with IDRISI (slopes, percentage cover, flowpaths etc.).

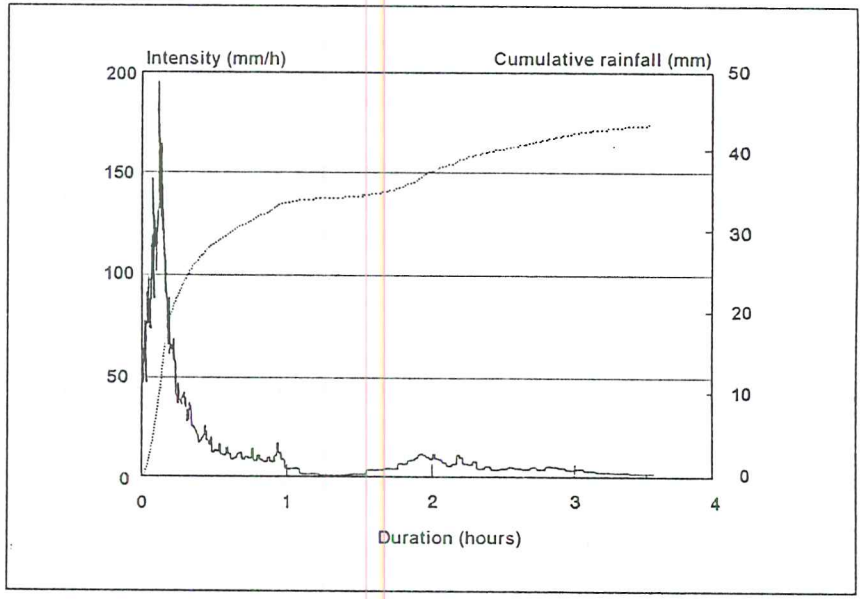

Figure 3. Intensity pattern of a typical shower in northern Burkina Faso (June 2, 1993).

Slopes in this watershed were classified in 5 classes (Table 2). The median slope of the watershed is 1.2 %.

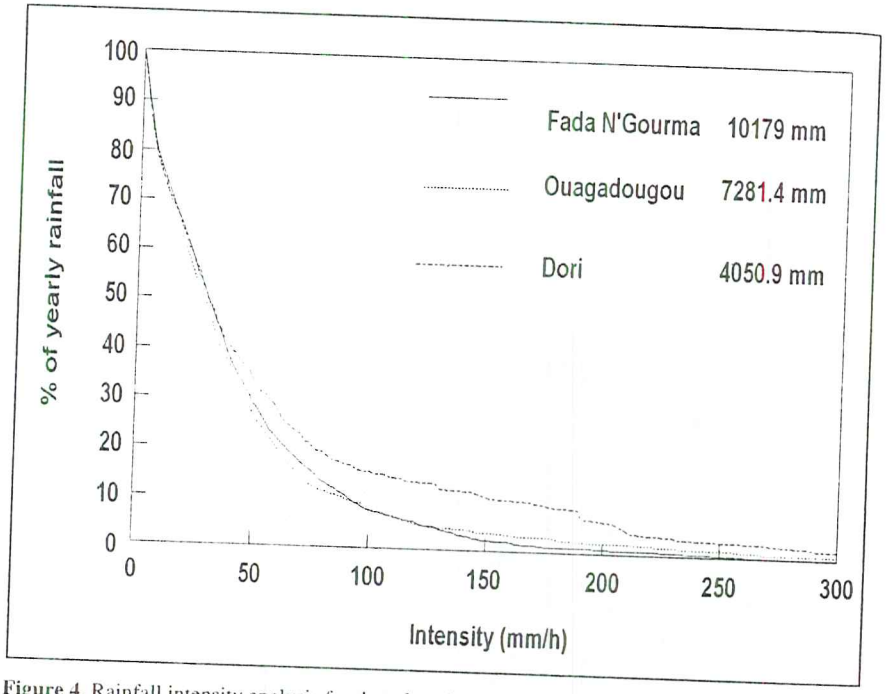

Figure 4. Rainfall intensity analysis for three locations in Burkina Faso.

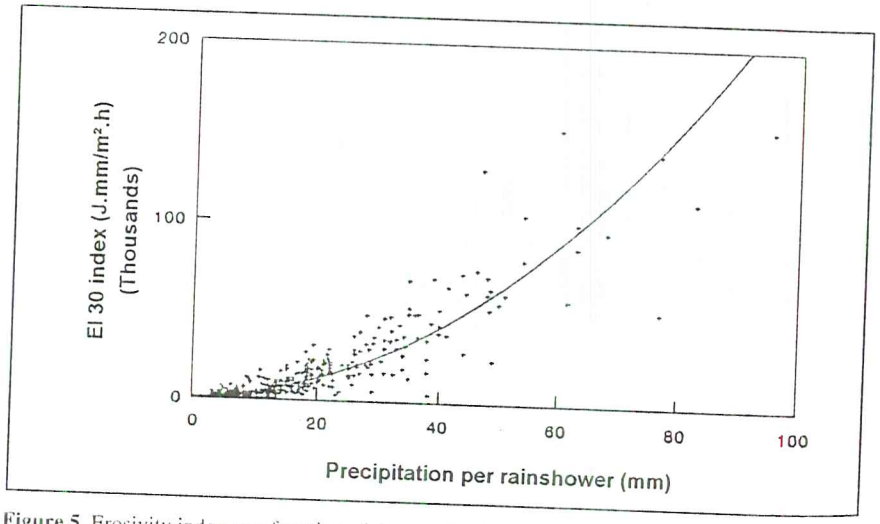

Figure 5. Erosivity index as a function of shower size for Burkina Faso.

Table 2. Typical slope classes for rangelands in northern Burkina Faso.

Slope class	% slope	% of watershed
1	< 1	40
2	1-2	33
3	2-3	15
4	3-5	6
5	> 5	6

3.2.2. Crust cover

Special attention was given to the *crust cover:* inventories were made on the basis of visual observations, using the classification as proposed by CASENAVE and VALENTIN (1989) as a guideline, and supported by measurements of the infiltration capacity. When degraded, glacis are partly bare and covered with 5 surface types:

1. Recent sandy dunes formed by deposition of aeolian sand. These small dunes are 10-50 cm high and cover an area of 2-20 m² and are often covered with rapid germinating pioneer vegetation. On this surface so-called drying crusts are found.
2. Older dunes where erosion has taken place, the soil surface contains more silt than the recent dunes, there is less vegetation cover and more algae growth. The algae crust type is a succession (in development) of the drying crust.
3. Crust on lateritic soil with gravel (laterite concretions) pavements.
4. So-called B-crusts which are supposed to be a succession of crust type 3 after removal of the protecting pavement.
5. Depositional (sedimentary) crusts are present in micro- as well as macro-depressions in 10% of the area.

Results of crust observations for Silmiougou are given in figure 6 and their classification according to their runoff properties into 6 classes (% runoff after 89 mm simulated rain shower) is presented in table 3. Class 1 represents arable land and classes 2-6 are sylvo-pastoral areas.

Table 3. Typical crust classes for rangelands in northern Burkina Faso and weighted mean runoff for a whole season and a design storm of 89 mm.

Crust class	% of watershed	% Runoff seasonal	% Runoff 89 mm
1	8	16	20
2	21	25	55
3	27	55	65
4	29	60	75
5	14	65	85
6	1	70	95
	Crust weighted mean runoff:	**49**	**64**

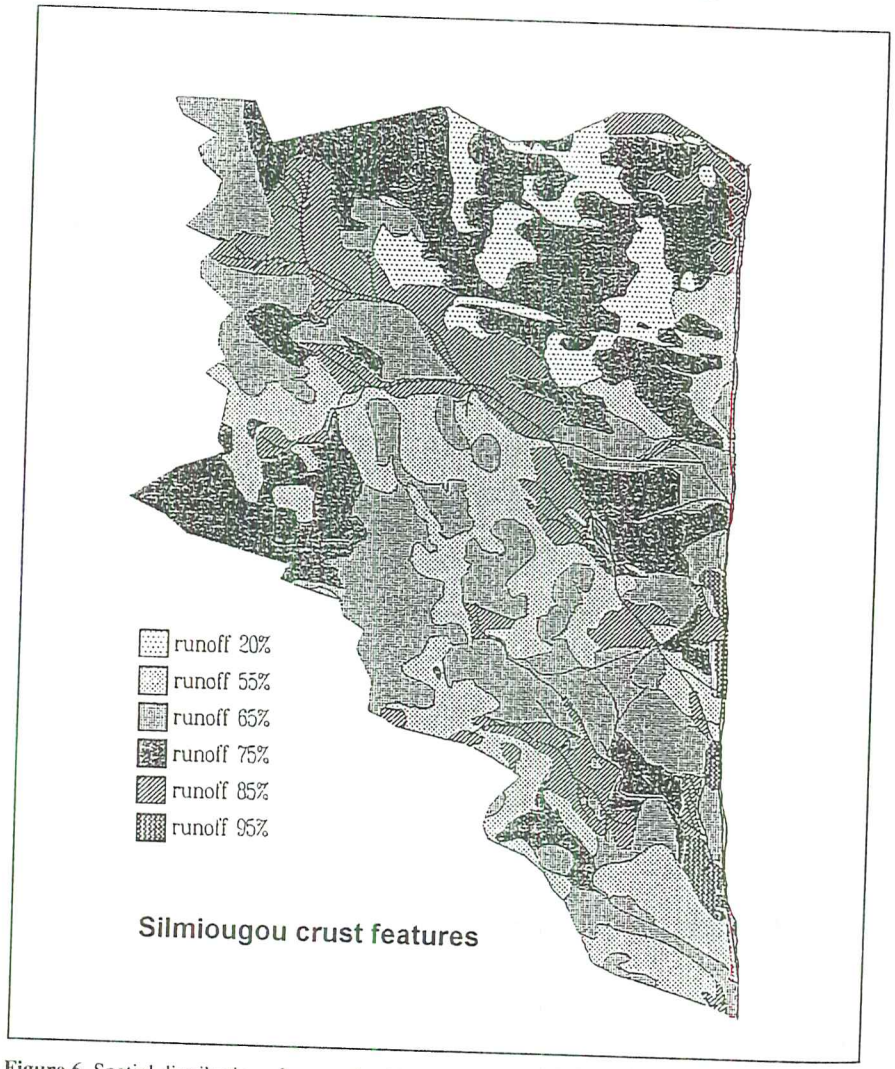

Figure 6. Spatial distribution of crusts classified according to their runoff behaviour.

3.2.3. Physical and chemical surface soil properties

With moisture retention curves and field capacity known, available water was calculated for the major surface soils in Table 4.

Table 4. Typical pF and available moisture data for 4 different crusted soils on rangelands in northern Burkina Faso.

	Soil Type	pF 2.0	pF 4.2	Available moisture (mm/mm)
1	Recent dunes	0.248	0.024	0.224
2	Older dunes	0.222	0.046	0.176
3	Laterite soil	0.267	0.107	0.160
4	B-crusted soil	0.280	0.189	0.091

Table 5 shows some physical characteristics of the soil underlying the most important crust types.

Table 5. Some physical and mechanical characteristics of the soil underlying the important crust types in Silmiougou.

Crust type	Tensile Strength (kPa)	Slump on Immersion (%)	Clay/Silt Ratio	% Sand (<53 :m)	% Gravel (> 2 mm)	Bulk Density (g/cm^3)
Drying crust on recent dunes	1,3	25	0,56	83	0,3	1,57
Algae crust on old dunes	28	19	0,62	68	0,3	1,59
Crust with gravel	89	39	1,43	47	48	1,74
B-crust	90	27	3,33	51	5	1,66

The sandy soils on which the drying and algae crusts have developed, show a high percentage of sand, a small amount of silt and a bulk density of just under 1.60, which is normal for these soils. The algae crusted soil has clearly collected more silt and clay material than the drying crust which becomes evident in the increased tensile strength and a lower slump percentage (less slump = more stable). The gravelly soil and the crusted soil where gravel has been removed are heavier (approx. 50% clay and silt). Their tensile strength is accordingly higher. This does not mean, however, that the fine material is more stable than sand: soil from the crust with gravel showed the lowest stability for the slump test.

This may explain why on this soil type, after removal of the protective gravel pavement, the crust becomes stronger and denser.

3.2.4. Runoff and erosion

Runoff as a result of natural rainfall from typical surfaces on the Silmiougou watershed was collected from small (1 m²) plots. These plots were made of sheet metal measuring 0.8 x 1.25 m (length along slope), with a collecting system consisting of an 80 l barrel, dug into the soil. In this way, only the total volume of runoff can be assessed.

Runoff of individual rain showers appeared to be well correlated with shower size (intensity mm/hr x duration in hours). Linear regressions with $R=aP-b$, in which R (mm) is the runoff and P (mm) the shower size, show high correlations. The higher a is, the better the correlation is. In the above equation is a the slope of the linear regression and often called the runoff coefficient and b the intercept with the dependent R-axis. This makes b/a (mm) the threshold rainfall volume above which runoff starts so that the above equation is only defined for $P > b/a$. Results for young and older dunes are given in figure 7 and for gravel pavement and structural B-crusts in figure 8. Regression results are given in table 6.

Table 6. Runoff formulas and runoff threshold values for typical surfaces on degraded sylvo-pastoral soils in northern Burkina Faso.

Main crust types	Runoff formula	Threshold (mm)	Corr
Drying crust	R=0.50*P 3.5	7.0	0.68
Algae crust	R=0.82*P 3.5	4.3	0.81
Crust with gravel	R=0.78*P3.5	4.5	0.92
B-crust	R=0.95*P 3.5	3.7	0.94

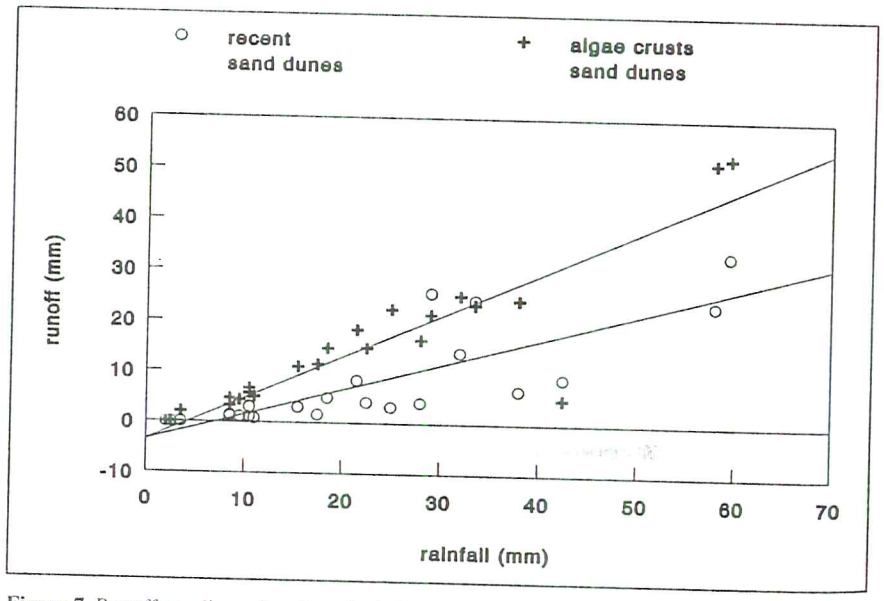

Figure 7. Runoff as a linear function of rainfall for recent and degraded (due to algae crust) sand dunes on Sahelian rangeland.

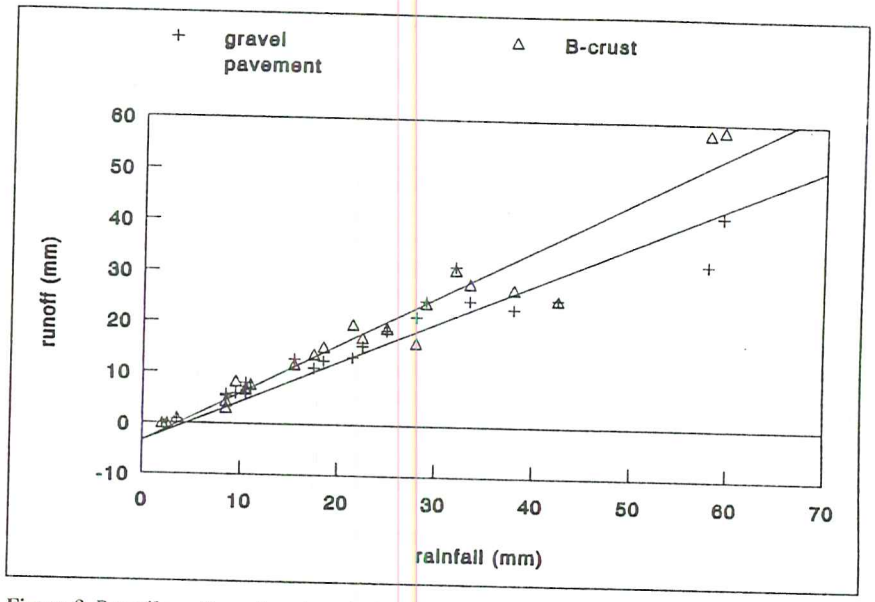

Figure 8. Runoff as a linear function of rainfall for degraded sylvopastoral soils with a gravel pavement (crust with gravel) and a B-crust.

The process of crust formation and resulting runoff was measured under a rainfall simulator (type Orstom) using a T-jet nozzle spraying water from a height of approx. 4 m on a 1 m² plot (1 x 1 m). The rainfall simulator tests yield a curve showing the decrease of infiltration rate as a function of time or cumulative rainfall. This study showed that crusts on Silmiougou soils develop rapidly, after being broken by tillage, under influence of cumulative rainfall (Figs 9 and 10), and that the rate of crust formation is strongly determined by the organic matter content of the soil.

Soil loss shows a poor correlation with shower size, shower intensity or erosivity. This is probably due to soil deposited on the experimental plots by wind erosion. Therefore, soil loss is often expressed in the units kg/ha.mm rain. For sylvopastoral land use, values range between 3 and 45 kg.ha.mm rain so that annual soil loss ranges between 2 and 30 t/ha.yr.

Plant nutrients are lost through soil loss as well as in the runoff water. In the runoff water we have measured in 1993 in Silmiougou about 40 g/ha.mm runoff of plant available N. The annual runoff of degraded sylvopastoral areas is about 50% so that at an isohyet of 650 [mm/yr], the runoff amounts to 325 mm/yr containing 13 kg_N/ha. The 650 mm of rain brings about 10 kg_N/ha so that the net loss due to runoff is 3 kg/ha.yr.

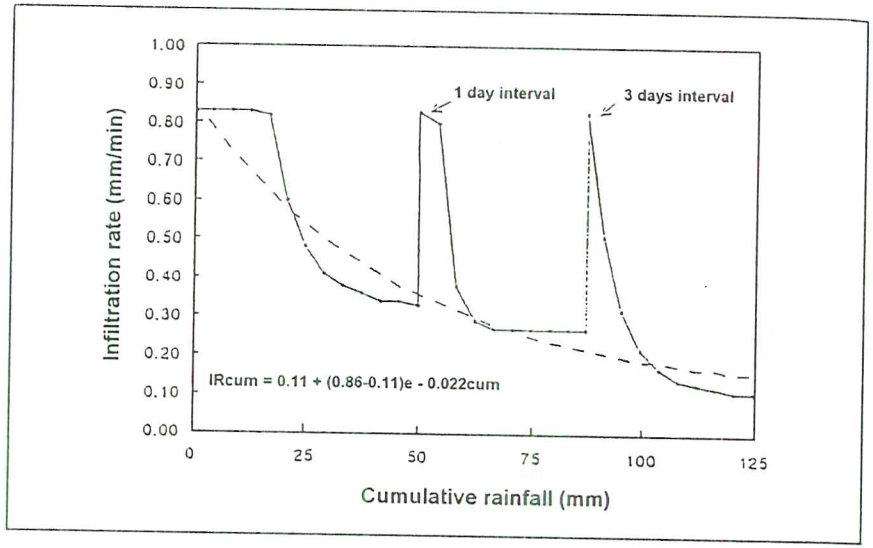

Figure 9. Infiltration rate as a function of cumulative rainfall after crust breaking for degraded sylvopastoral soils with only 0.24% soil organic carbon (1 or 3 days interval).

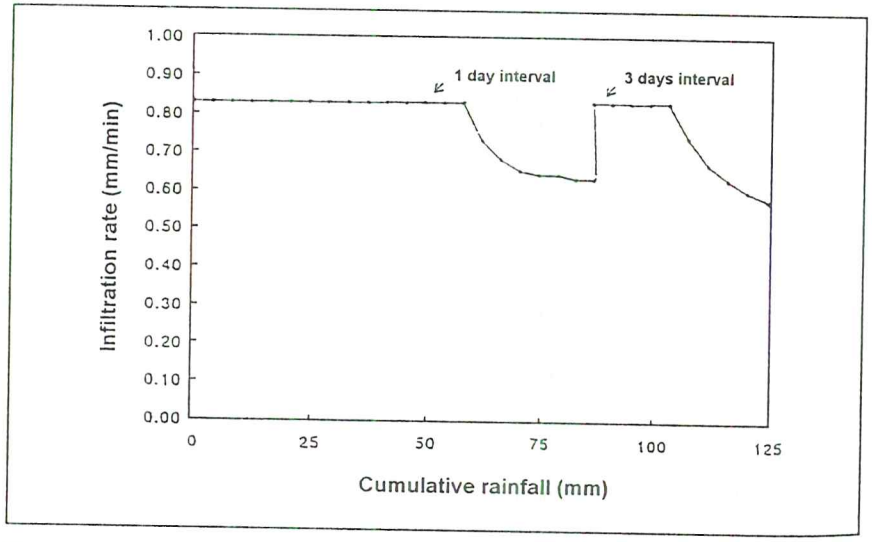

Figure 10. Infiltration rate as a function of cumulative rainfall after crust breaking for agricultural soils with 1.24 % soil organic carbon.

Nutrient erosion can be expressed in terms of total elements or in terms of available nutrients, both methods have pros and cons. Results show that the majority of the total elements is in the eroded sediment while the majority of the plant available nutrients is in the runoff water (see table 7). Effects of long-term gradual nutrient loss on yield and the costs and benefits of conservation technology have been calculated. Taking into account the nutrient conserving function of certain soil conservation methods can make this technology economically viable.

Table 7. Distribution of annual losses of nutrients (kg/ha.yr) between sediment and runoff for two types of land use on degraded sandy loam soils in Burkina Faso (1994 data).

	Sylvopastoral			Agricultural		
	Sediment	Runoff	% in sediment	Sediment	Runoff	% in sediment
C	118	23	84	361	17	96
Total N	13	7	67	28	14	67
Avail N	0.2	6.6	3	0.2	13.7	2
Total P	1.5	0.0	100	4.8	0.1	99
Avail P	0.0	0.0	–	0.0	0.1	0
Avail K	1.1	3.3	25	1.1	7.6	13

The eroded sediment always contains higher concentrations of organic matter and nutrients than the topsoil from which it originates. This phenomenon is called enrichment. The ratio between the concentration of an element in the sediment to that in the soil is called the enrichment factor (*indice de sélectivité*). Enrichment factors for total elements are higher (2-4) than for available nutrients (1-2), see table 8.

Table 8. Chemical analysis of the original soil, the erosion sediment and runoff for two types of land use on degraded sandy loam soils in Burkina Faso.

	Sylvopastoral				Agricultural			
	Soil	Sediment	Enrichment	Runoff	Soil	Sediment	Enrichment	Runoff
C (%)	0.6	2.1	3.5	-	0.7	1.7	2.4	-
TOC (ppm)	-	-	-	6.0	-	-	-	5.4
Total N (%)	0.06	0.24	4.0	-	0.05	0.13	2.6	-
Avail N (ppm)	42	-	-	1.67	7	10.3	1.5	2.95
Total P (ppm)	105	277	2.6	-	75	219	2.9	-
Avail P (ppm)	0.44	-	-	0.00	0.02	-	-	0.01
Avail K (ppm)	94	-	-	0.80	53	50.3	0.95	1.56
pH	6.5	-	-	-	6.2	-	-	-

- : no data available. Note: TOC (Total Organic Carbon) determines 82% of C determined with Kurmies.

One can use the runoff relations in combination with crust areas for upscaling the information towards the watershed scale. This is especially important for the design of Soil and Water Conservation technology. For that case one uses not only an average seasonal rainfall distribution but also a so-called design rain shower. This is the shower with an occurrence chance of once in ten years which is for Silmiougou 89 mm. By multiplying the relative contributions of the various crust surfaces with their respective runoff coefficients one obtains a seasonal runoff of 49% of 650 mm and a design runoff of 64% of the 89 mm design storm (see also table 3). This latter value is compared with the Orstom-method for the calculation of the design discharge:

$$V_{10} = P_{10} \cdot A \cdot Kr \cdot S$$

In which: V_{10} is the 1 in 10 years design discharge, P_{10} is the 1 in 10 years design precipitation (89 mm based on 30 years of records), A reflects the size of the watershed (A = 1 for < 25 km²), S is the permeability class of the watershed and Kr is a factor for vegetation cover (1 for degraded Sahelian vegetation). For a choice of permeability class P2 = 0.75, for slope class R3, V_{10} = 8,344 m³ which implies a runoff percentage of 75% or if P3 = 0.35 is chosen V_{10} = 3,894 m³ and the runoff is 35%. The above calculated crust weighted mean of 64% is in between these values.

The following students of the Agricultural University of Wageningen have contributed in the period 1992-1995 to the results presented here (their reports are available at the *Antenne Sahélienne* in Ouagadougou): A. BLEUMINK, L. COOLEGEM, K. VAN DIJK, R. GEELHOED, M. DE HAAS, I. JANSSEN, S.J.T. POUTSMA, M. RIETKERK, B. TAMMES, J.D. WIJNHOUT, A.J. OTTO and A. DE WIT.

4. Excursion

The route Ouagadougou - Kaya is given in figure 11.

4.1. Outcrops of granite and porphyroïdic granite near Ziniaré

4.2. Baobab trees in the conservation forest of Bissiga

The Baobab tree or *Andosonia digitata* belongs to the *Bombaceae* family and is characterized by: great height, alternating leaves and capsulated fruit. The holes inside of the trunks are often occupied by wild animals.

The tree plays a cultural, social and economic role in the society. It is believed to be occupied by spirits and is used as worship area. The area under the tree is used as meeting zone for old men. Its products are used for feeding, medicines, rural chemistry and cooking tools.

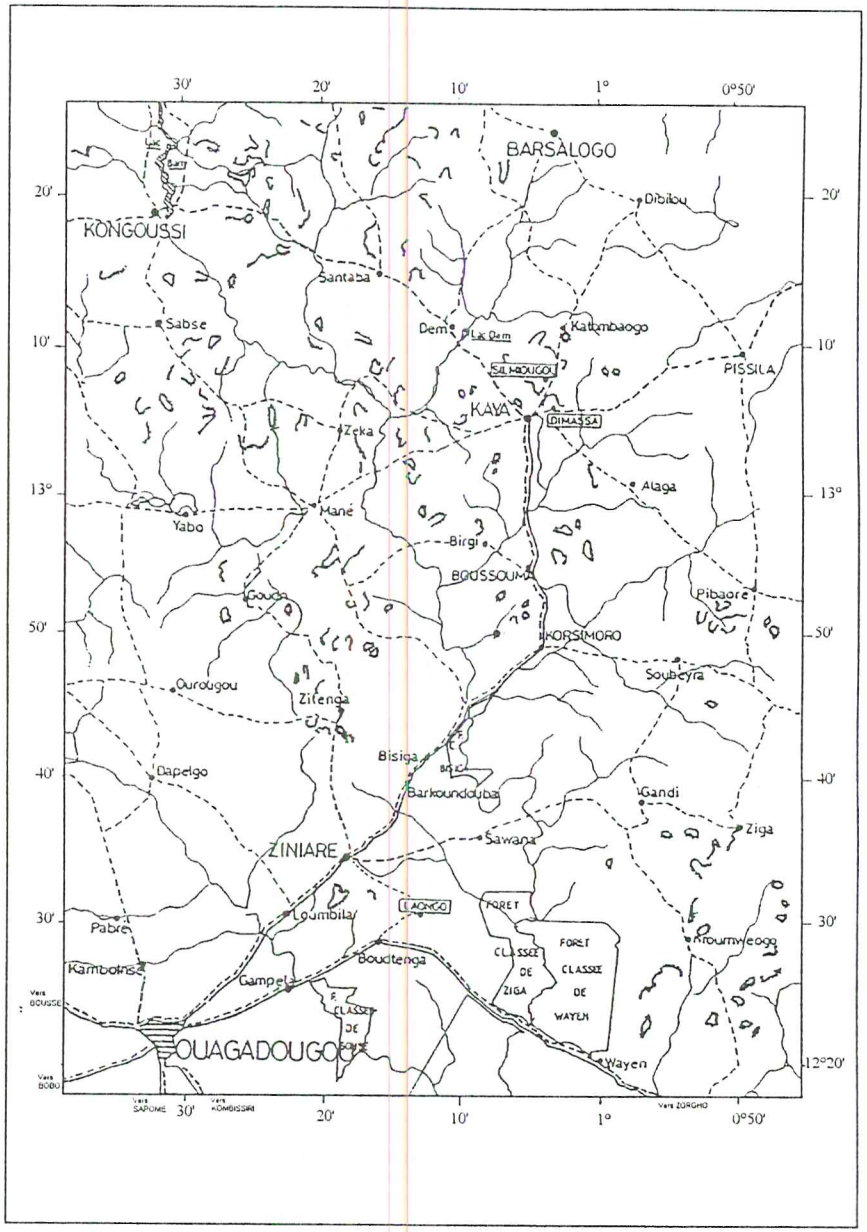

Figure 11. Topographic map showing the excursion route.

4.3. Green schist and dolerite of the Birrimian

4.4. Eroded zone of Dimassa

4.4.1. Demonstration of remote sensing imagery and physiographic map of the Kaya region

In the area, two geologically defined landscapes are found:
- Schist and meta-volcanites;
- Granite and migmatite.

A further subdivision is done on the physiographic map, showing toposequences from high to low: schist hills and ironcapped plateaus, steep slopes, colluvial footslopes, faint slopes of the valley and valley bottoms. The ironcapped plateaus are clearly marked on Landsat TM imagery, while the valley bottoms show up by their more dense tree vegetation.

4.4.2. Demonstration of the Mini-IRIS field spectrometer

This is a single field of view instrument, so a reference plate has to be used to determine the incoming solar radiation. The instrument measures in 140 wavelength bands between 400 nm and 2,500 nm.

For the use of field reflectance to explain the reflected radiance, registered by the satellite, the correlation between the two should be high. An example of this relation is given in figure 12. Different spectral curves measured in the Kaya region are given in figure 13.

4.4.3. Soil profile (92-4 bis): Eutric Fluvisols or Sols peu évolués d'apport alluvial sur Sols ferrugineux tropicaux lessivés

Sedimentary cover derived from granite weathering and transported by runoff and wind, lying over an Early Holocene truncated B2t horizon with brown and red mottles at 80 cm soil depth. Profile situation: valley with nearby granite outcrops.

For soil analyses of profile 92-4, located at 100 m distance at the side of gullied land, the reader is referred to Table 9. The soil horizon in this profile at a depth of 81-120 cm (representing a truncated Bt horizon) is rich in iron concretions; a hardened ironstone layer is found at greater depth.

4.5 Soil profile (93-1) near Silmiougou: Eutric Cambisol or *Sol brun eutrophe tropical*

A soil extending up to 55 cm depth with a cambic horizon, developed on schist exposed on a footslope.

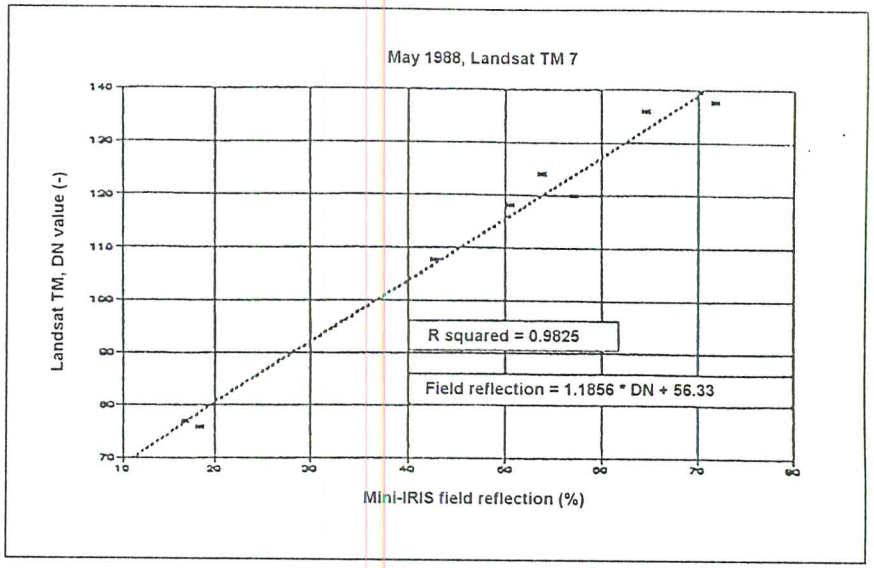

Figure 12. Regression between Landsat TM7 and the Mini-IRIS.

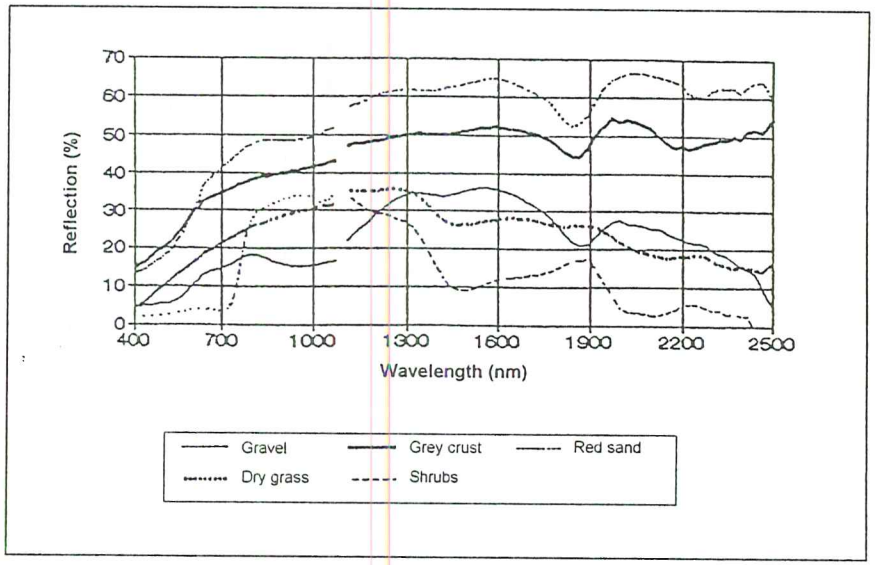

Figure 13. Different spectral curves of surfaces in the Kaya region, measured with the Mini-IRIS.

4.6 Soil profile (92-2) near Silmiougou: Luvic Arenosols or *Sols minéraux bruts d'apport alluvial sur Sols ferrugineux tropicaux lessivés*

Sedimentary cover derived from granite weathering and transported by runoff and gullies, lying over an Early Holocene truncated B2t horizon with brown mottles at 90 cm soil depth. Profile situation: valley with nearby gully. For analytical data of sedimentary cover, see table 9.

Discussion on soil classification

A dispute arose about the following: although the plant has to extract most of the nutrients of the young sedimentary cover in the profiles 92-4bis and 92-2, the FAO-UNESCO Legend of the Soil Map of the World would force the classification of Luvisols. Furthermore, material transported over short distances by water in gully systems (*ravinement*) is regarded by most experts as colluvium. However, others claim a fluvic character for the same deposit.

In the criteria for classification of the Soil Map of the World, it is stated that if horizons are buried by 50 cm or more of newly deposited surface material, they are no longer diagnostic for classification purposes. This means that in both cases (92-4bis and 92-2), the soils have to be classified according to the characteristics of the sedimentary cover.

Is the material fluvic ? The organic matter content remains at 0.2% for the upper 89 cm of soil in profile 92-2. For profile 92-4bis, it remains at 0.2% for the upper 23 cm and between 81 cm and 120 cm, while it is above this value between 45 cm and 81 cm. There is some stratification but less than 25 % of the soil volume. Conclusion: the material of profile 92-4bis has to be regarded as fluvic owing to the irregular distribution of organic matter with depth. The material of 92-2, however, does not fulfil the carbon requirements to be considered fluvic.

The soil profile 92-4bis was arbitrarily classified as Luvic Arenosols in having clay accumulation within 125 cm of the surface. Arbitrarily, since the clay illuviation took place in a truncated buried soil.

Postexcursion, the mineralogical and chemical composition was determined. For this purpose, 4 types of soil material were sampled (between brackets, abbr. in tables 10 and 11):

- Schist derived soil (*schder*);
- Sedimentary cover of mixed origin in schist and meta-volcanites landscape (*mixsch*);
- Mottled subsoil in the granite and migmatites landscape (*subgran*);
- Sedimentary cover in the granite and migmatites landscape (*sedgran*).

X-ray diffraction of the soil fraction < 2 mm showed the mineralogical composition to be: dominantly quartz, common kaolinite, some feldspar; sample 92-4 (23-45 cm) was very rich in quartz. The schist-derived soil contained in addition: smectite and a little goethite. The latter was also present in sample 92-2 (100-105 cm).

Table 9. Soil analyses 92-2 and 92-4 (BUNASOLS, National Soils Bureau).

Soil analyses	92-2	92-2	92-4	92-4	92-4	92-4	92-4	92-4
Soil depth (cm)	6-43	43-89	4-11	11-23	23-45	45-61	61-81	81-120
Texture class	ls	ls	ls	s	ls	sl	sl	l
< 2 µm	7.5	8.3	7.5	6.3	7.5	17.5	16.8	26.8
2-50 µm	9.6	6.5	6.5	7.3	10.2	16.3	16.3	12.5
50-100 µm	27.8	20.1	27.8	28.9	21.5	17.6	26.4	20.1
100-250 µm	28.5	27.2	29.9	36.7	22.5	18.7	20.1	17.0
250-2000 µm	26.6	37.3	28.3	20.8	38.4	20.0	20.4	23.7
C_{total} (%)	0.2	0.2	0.2	0.2	0.2	0.4	0.3	0.2
$CaCO_3$ (%)								1.8
pH_{water} 1:2.5	5.9	6.2	5.4	5.8	5.4	4.9	5.3	7.0
pH_{KCl} 1:2.5	4.4	4.7	4.1	4.4	4.4	4.0	4.5	5.8
Exch. H^+ (meq/100 g)			0.5		0.3	0.8	0.5	
$P_{Ass.}$ (ppm)	2.2	1.6	1.3	1.7	0.6	1.6	0.9	5.4
K_{total} (ppm)	53.5	34.9	11.8	9.2	8.4	9.8	9.2	20.6
P_{total} (ppm)	76.6	38.3	38.3	38.3	38.3	95.7	76.6	95.7
Free Fe_2O_3	1.2	0.3	1.0	0.8	1.0	1.6	1.6	1.5
Exch. Bases (meq/100 g)								
Ca^{2+}	1.5	1.7	1.3	1.3	1.6	2.9	3.0	5.2
Mg^{2+}	0.4	0.4	0.4	0.4	0.5	1.1	0.8	1.2
K^+	0.2	0.1	0.0	0.0	0.1	0.0	0.0	0.1
Na^+	0.2	0.1	0.1	0.1	0.3	0.2	0.1	0.1
Sum of bases	2.3	2.2	1.7	1.9	2.5	4.1	3.9	6.5
CEC (meq/100 g)	7.3	6.0	9.0	5.1	4.4	5.8	7.3	8.3
Base saturation (%)	31.4	38.8	18.7	36.5	56.6	70.7	54.1	

Evidence for differentiation between the 4 types of material was found by X-ray fluorescence spectrometry (Tables 10 and 11).

Considering the sedimentary cover in the granite and migmatites landscape (*sedgran*), this material was found to be for the greater part derived from granitic rock, witness its composition (Table 10). The mottled subsoil (*subgran*) is different from its sedimentary cover, showing some influence of schist and metavolcanic material (*schder*, Table 10).

The sedimentary cover of mixed origin in the schist and metavolcanites landscape was found to be intermediate between the mottled subsoils (*subgran*) and schist derived soil or between granite and schist derived soil.

Table 10. Results of XRFS-analysis for major and minor components (WAU, Soil Science and Geology).

Samples	Soil depth (cm)	SiO_2 (%)	Al_2O_3 (%)	Fe_2O_3 (%)	TiO_2 (%)	K_2O (%)	MgO (%)	CaO (%)	MnO (%)	P_2O_5 (%)
schder										
93-1	50-55	66.75	12.18	8.38	1.21	0.49	1.04	1.50	0.13	0.06
mixsch										
92-3	9-40	83.57	7.89	3.53	0.75	0.65	0.26	0.10	0.04	0.03
92-3	40-54	85.68	8.35	3.48	0.78	0.65	0.22	0.08	0.05	0.03
92-3*	40-54	80.54	8.31	3.52	0.76	0.65	0.24	0.08	0.05	0.03
92-3	54-77	83.45	8.53	3.50	0.80	0.64	0.25	0.09	0.04	0.03
92-3	77-110	81.75	9.37	3.89	0.83	0.68	0.26	0.09	0.04	0.03
subgran										
92-4	81-120	76.57	11.06	3.95	0.59	0.81	0.24	0.07	0.04	0.02
92-4*	81-120	76.69	11.10	3.97	0.63	0.80	0.23	0.08	0.04	0.02
92-2	100-105	70.99	12.48	6.84	0.75	0.70	0.28	0.07	0.01	0.02
92-2*	100-105	71.53	12.48	6.83	0.73	0.69	0.29	0.07	0.01	0.02
93-4b	100-105	79.80	9.34	3.26	0.55	0.82	0.29	0.17	0.03	< 0.01
sedgran										
92-4	23-45	90.59	5.09	1.87	0.44	0.85	0.14	0.05	0.02	< 0.01
92-4	45-61	83.13	8.66	2.60	0.54	0.96	0.24	0.08	0.03	0.02
92-4	61-81	84.04	8.34	2.53	0.52	0.87	0.17	0.04	0.02	0.02

* duplo. Other abbreviations: *schder*: schist derived; *mixsch*: sedimentary cover of mixed origin in schist and metavolcanites landscape; *subgran:*:mottled subsoil in granite and migmatites landscape; *sedgran:*sedimentary cover granite and migmatites landscape. Rem : 92-3 was not visited during excursion.

Although weaker in evidence, the results on trace elements support these findings in most instances (Table 11).

Thin sections were studied by Dr. Ing. A.G. JONGMANS of the Laboratory of Soil Science and Geology (Wageningen Agricultural University). The results were as follows:

- Sample 92-2 (100-105 cm; *subgran*) had about 3 % argillans with many silica accumulations as result of ferrolysis;
- Sample 92-4 bis (100-105 cm; *subgran*) showed 1 % argillans with few silica accumulations as result of ferrolysis;
- Sample 93-1 (50-55 cm; *schder*) showed stress cutans (skelsepic and glaesepic) but no sign of ferrolysis.

The presence of illuvial concentration in the mottled subsoil of the granite and migmatites landscape is proved by these results. The results point to a soil forming process under more humid conditions than today, witness the ferrolysis. Such conditions existed in the area during the Early Holocene.

Since the presence of new material on top of these horizons is proved, the soil profile 92-4bis is classified as Eutric Fluvisol in having a sedimentary cover with fluvic character and a base saturation of 50 percent or more at least between 20 cm and 50 cm from the surface (neglecting 20-23 cm with low base saturation in 92-4, Table 9), lying over an horizon with clay accumulation at a depth of more than 50 cm.

Table 11. Results of XRFS analysis for trace elements (WAU, Soil Science and Geology).

Samples	Soil depth (cm)	Zr (ppm)	Ba (ppm)	V (ppm)	Cr (ppm)	Sr (ppm)	Cu (ppm)	Ni (ppm)	Rb (ppm)	Nb (ppm)	Pb (ppm)	Co (ppm)	Ga (ppm)
schder													
93-1	50-55	444	279	280	84	79	113	52	32	34	17	28	23
mixsch													
92-3	9-40	519	200	158	63	47	48	40	37	34	19	25	18
92-3	40-54	516	225	159	61	50	59	34	38	33	20	17	19
92-3	54-77	522	210	153	52	45	45	35	37	31	16	11	21
92-3	77-110	539	209	178	60	49	57	41	42	35	20	14	20
subgran													
92-4	81-120	445	394	123	53	79	52	30	52	26	18	<10	21
92-2	100-105	410	286	163	91	76	49	28	43	27	26	<10	23
93-4b	100-105	474	410	112	51	97	49	26	42	24	19	10	20
sedgran													
92-4	23-45	527	335	90	40	75	35	49	32	32	16	31	15
92-4	45-61	451	356	108	40	75	45	30	47	29	15	14	18
92-4	61-81	508	358	106	41	73	39	38	40	29	19	19	18

For abbreviations on samples: see table 10. 92-3 was not visited during the excursion.

The soil profile 92-2 is classified as Haplic Arenosol in having a sedimentary cover of coarse texture and lacking fluvic properties; it also covers an horizon with clay accumulation at a depth of more than 50 cm.

This classification does justice to the fact that the upper 50 cm of soil is most important for plant growth and classification should reflect the genesis of that part of soil. However, it is regrettable that the presence of B2t horizons in the subsoil is not reflected in the class name.

Also, the geological term "colluvium" would be misused if applied to the deposits under consideration. Besides some minor aeolic influence, these are deposited after short fluviatile transport in an active eroding and accumulating environment. The French terms *"ruissellement"* and *"ravinement"* are most appropriate for this. In this environment, only locally periods of soil formation are long enough to produce A-horizons with organic carbon contents of more than 0.2%.

The French soil classification system (CPCS, 1967) gives no solution for the classification of polygenetic soil profiles since the lower limit of newly deposited material on top of old soil material is not defined. Taking the same criterium of the Soil Map of the World (50 cm thickness), the two profiles (92-4bis and 92-2) have to be classified as: *Sols peu évolués d'apport alluvial.* To do justice to profile development, the addition is given: *sur Sols ferrugineux tropicaux lessivðs* (subgroup *induré* for profile 92-4bis).

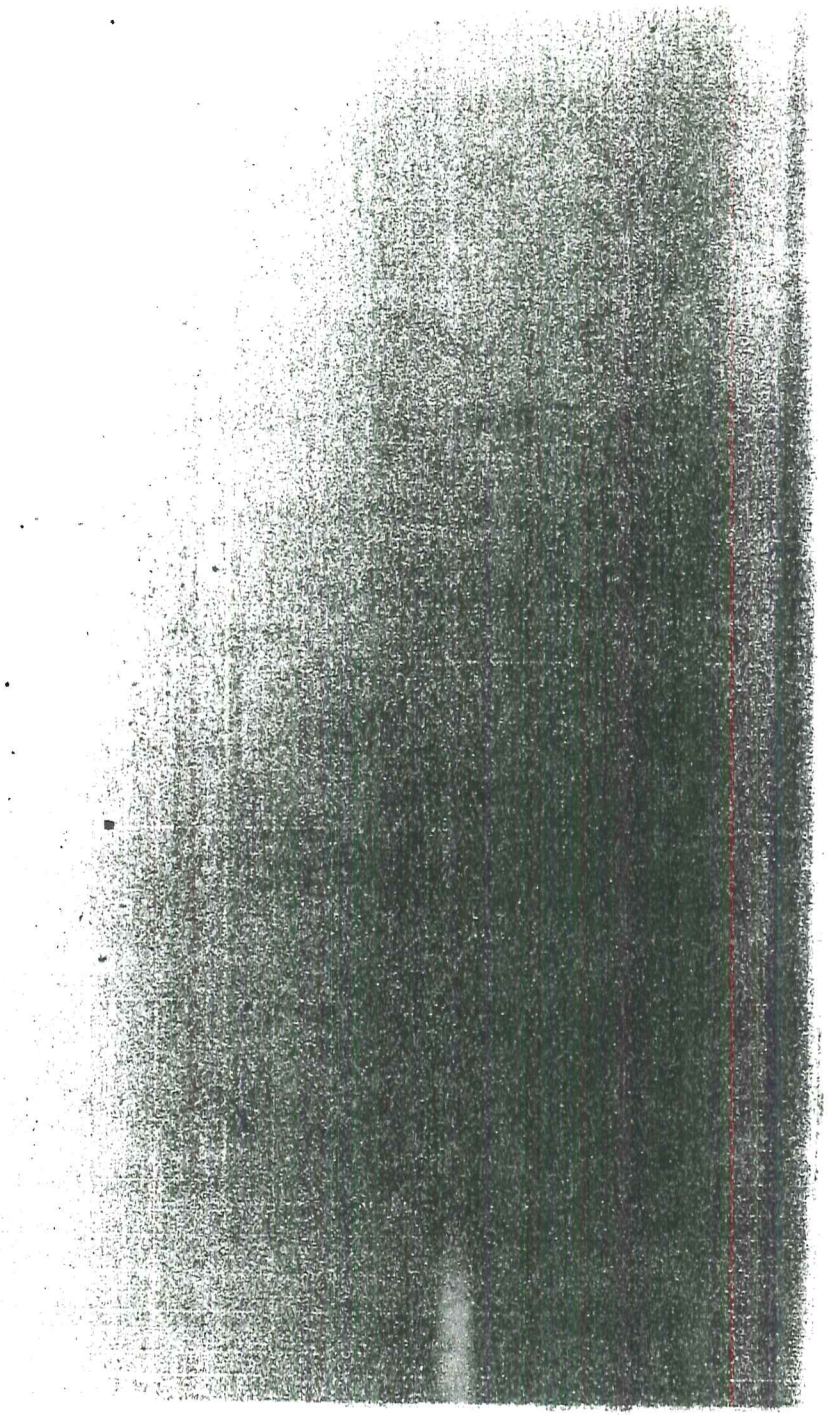

4.7. Visit to degraded watershed of Silmiougou (for data, see 3.2)

4.8. Panoramic view from an ironcapped plateau edge

The ironcap is regarded to be from Pleistocene origin. At many places, a thin aeolic cover is found where vegetation offered a take hold for the sediment.

The different maps of the Kaya region were presented and discussed at this place, maps on drainage pattern, physiography, land use and soils. These maps were derived from aerial photo-interpretation, satellite image interpretation (a.o. NDVI) and were used in GIS for further combination to arrive at erosion hazard estimates.

The discussion focused on land capability and development strategies.

PUBLICATIONS PARUES (depuis le 1er janvier 1995):

Publications de l'Antenne (vert)

19	J. de Graaff L. Stroosnijder	L'évaluation économique des mesures CES au Sahel (présenté lors des 11ème Journées du Réseau Erosion "L'environnement humain de l'érosion, 20-22 septembre 1994, ORSTOM/E.N.S. St. CLOUD-Université PARIS VII)
20	E. H. van Haaften F.J.R. van de Vijver	Psychological consequences of environmental Degradation
21	L. Stroosnijder	Quantification of nutrient erosion; Conference on Erosion and Land Degradation in the Mediterranean
22	K.F. Wiersum & B.E.J.C. Lekanne	The Forestry Agent at the Interface Between Local-Level Environmental Management and External Policies: Reflections on Forestry Interventions in the Sahel. In: Local Resource Management in Africa (van den Breemer, Drijver and Venema, ed.)
23	F.G. Hien M. Rietkerk L. Stroosnijder	Soil Variability and Effectiveness of soil and Water Conservation in the Sahel. Submitted to: Arid Soil Research and Rehabilitation.
24	N. de Ridder H. van Keulen	Estimating biomass through transfer functions based on simulation model results: a case study for the Sahel. In: Agricultural water management 28 (1995) 57-71.
25	B.E.J.C. Lekanne	Social Diversity, Intervention and Common Property Resources; Mossi villages and land management (Burkina Faso). Paper for the `Fifth Common Property Conference: Reinventing the Commons'. 24-28 May 1995, Bodo, Norway.
26	D. Niemeijer	The Dynamics of African Agricultural History: Is it Time for a New Development Paradigm? In: Development and Change, 27(1):87-110.
27	B. Ouedraogo	Le Forgeron, la Potière et le Teinturier face à la Crise de l'Environnement à Bangasse et à Tangasco. In: Droit et Cultures, 30, 1995.
28	L.A. Timmer, J.J. Kessler, M. Slingerland	Pruning of néré trees (Parkia biglobosa (Jacq.) Benth.) on the farmlands of Burkina Faso, West Africa. In: Agroforestry Systems 33: 87-98, 1996.
29	H.C.C. Meertens L.O. Fresco W.A. Stoop	Farming systems dynamics: Impact of increasing population density and the availablity of land resources on changes in agricultural systems. The case of Sukumland, Tanzania. In: Agriculture Ecosystems & Environment 56 (1996) 203-215.
30	M. Slingerland	Mulching in Burkina Faso. In: Indigenous Knowledge and Development monitor, Volume 4, Issue 2, August 1996, pp 3-5.
31	M. Slingerland, M. Masdewel	Mulhing on the central plateau of Burkina Faso. In: Sustaining the soil. Indigenous Soil and Water Conservation in Afrika. Chris Reij, Ian Scoones and Camilla Toulmin (eds), chapter 10: 85-89,1996.
32	M. Rietkerk, P. Ketner, I. Stroosnijder, H.H.T. Prins	Sahelian Rangeland development; a catastrophe? In: Journal of range Management 49(6), November 1996. p. 512-519.
33	M. Slingerland	
34	M.A. Mulders, M.C. Girard M.A. Mulders	Remote Sensing of Soils in Warm Arid and Semi-Arid Lands. In: Remote sensing reviews, 1993, Vol 7., p. 39- 49. Soil and Land Use Surveys. Inb: Encyclopedia of Agricultural Science, 1994, Vol. 4, p. 341- 363.

AUTRES PUBLICATIONS

- Hien, F.G. (1995). La régénération de l'espace sylvo-pastoral au Sahel: Une étude de mesures de conservation des eaux et des sols au Burkina Faso. Tropical Resource Management Papers No. 7, WAU, Wageningen, Pays-Bas.
- Kessler, C.A., W.P. Spaan, W.F. van Driel et L. Stroosnijder (1995). Choix et modalités d'exécution des mesures de conservation des eaux et des sols au Sahel. Tropical Resource Management Papers No. 8, WAU, Wageningen, Pays-Bas,94p.
- Zeeuw, F. de (1995). Sécurité foncière et gestion des ressources naturelles dans la Boucle du Mouhon - Burkina Faso. Tropical Resource Management Papers No. 9, WAU, Wageningen, Pays-Bas, 45 p.
- Kiepe, P. (1995). No Runoff, No Soil Loss: soil and water conservation in hedgerow barrier systems. Tropical Resource Management Papers No. 10, WAU, Wageningen, Pays Bas.
- Slaats, J. (1995). Chromolaena odorata fallow in food cropping systems; an agronomic assessment in South-West Ivory Coast. Tropical Resource Management Papers No. 11, WAU, Wageningen, Pays-Bas.
- Reuler, H. van (1996). Nutrient Management over Extended Cropping Periods in the Shifting Cultivation System of south-west Côte d'Ivoire. Tropical Resource Management Papers No. 12, WAU, Wageningen, Pays-Bas.
- Oneka, M. (1996). On Park Design: looking beyond the wars. Tropical Resource Management Papers No. 13, WAU, Wageningen, Pays Bas.
- Graaff, J. de. (1996). The Price of Soil Erosion: an economic evaluation of soil conservation and watershed development. WAU, Wageningen, Pays Bas.